A data-driven approach for ship-bridge collision candidate detection in bridge waterway

Zhang, Liang; Chen, Pengfei; Li, Mengxia; Chen, Linying; Mou, Junmin

DOI
10.1016/j.oceaneng.2022.113137

Publication date
2022

Document Version
Final published version

Published in
Ocean Engineering

Ocean Engineering 266 (2022) 113137

Contents lists available at ScienceDirect

Ocean Engineering

journal homepage: www.elsevier.com/locate/oceaneng

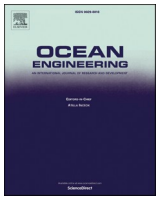

A data-driven approach for ship-bridge collision candidate detection in bridge waterway

Liang Zhang [a,b], Pengfei Chen [a,b], Mengxia Li [a,b,c,*], Linying Chen [a,b], Junmin Mou [a,b]

[a] School of Navigation, Wuhan University of Technology, Wuhan, China
[b] Hubei Key Laboratory of Inland Shipping Technology, Wuhan, China
[c] Safety and Security Science Group, Faculty of Technology, Policy and Management, Delft University of Technology, Delft, the Netherlands

ARTICLE INFO

Keywords:
Collision candidate detection
Ship-bridge collision avoidance
Data-driven
Kernel density estimation
Velocity obstacle

ABSTRACT

The consequences caused by bridge failures owing to the ship-bridge collision are always severe in terms of loss of life, economy, and environmental consequences to individuals and societies. The previous studies focused on the ship-bridge collision mainly concentrated on passive anti-collision, such as strengthening the bridge structure or setting anti-collision facilities. Compared with the previous research, the contribution of this work is to facilitate the reduction of collision risk of ship-bridge collision from the perspective of active anti-collision. A data-driven approach for ship-bridge collision candidate detection method in inland bridge waterways is proposed in this research. The approach is mainly divided into two steps: 1) The features (channel boundary, pier domain, and ship domain) of bridge waterways are identified using Kernel Density Estimation (KDE) method based on the historical AIS data; 2) Collision candidate detection with Velocity Obstacle (VO) method considering the identified features. This work can provide beneficial support for the ship-bridge active collision avoidance system.

1. Introduction

Inland navigation is an important part of the comprehensive transportation system of China and plays an indispensable role in economic development. The Yangtze River has been the busiest inland waterway in the world, with a total length of 2838 km, and flows through 11 provinces. In the wake of the development of modern cities, 140 bridges have been built on the Yangtze River. With the increase in the number of bridges, more and more bridge collapse events caused by ship collisions happened. The losses caused by bridge failures due to the ship-bridge collision are always enormous, e.g. loss of life, economic and social consequences. The advanced analyses to mitigate the losses of ship-bridge collisions have attracted much attention.

In response to such attention, various methods have been proposed to minimize or eliminate the losses, which mainly from the perspective of passive anti-collision to provide effective protection from the damage to the bridge induced by the ships, such as strengthening the bridge structure or setting anti-collision facilities. It can effectively mitigate the damage to the bridge when the ship-bridge collision happened, but the probability of collision did not decrease. Moreover, once the impact force exceeds the load of bridge structures or anti-collision facilities, the role of protective measures is very limited. Hence, it is of great significance to carry out research from the perspective of reducing the ship-bridge collision probability.

In recent years, collision candidate detection, one class method for detecting potential collision risk, has attracted much research interest. Such methods consider the occurrence of certain non-accident events in the traffic system as safety performance indicators from Automatic Identification System (AIS) data. Due to restricted navigable conditions and high traffic density, there are many potential collision risks in the bridge waterways. It's helpful to decrease the probability of collision between ship-bridge by analyzing these risks. Nevertheless, fewer studies focused on collision candidate detection of bridge waterways for complex navigation features. This paper aims to perform collision candidate detection in the bridge waterways by considering the coupling effect of all navigation features.

The contribution of this paper is two-fold: 1) The paper proposed an approach for collision candidate detection in bridge waterways from the perspective of active anti-collision. It contributes to facilitating the reduction of collision probability of ship-bridge collision, and lays a foundation for decision support system of ship-bridge collision avoidance; 2) The collision candidate detection method proposed in this paper

* Corresponding author. School of Navigation, Wuhan University of Technology, Wuhan, China.
E-mail address: limengxia@whut.edu.cn (M. Li).

https://doi.org/10.1016/j.oceaneng.2022.113137
Received 10 April 2022; Received in revised form 6 September 2022; Accepted 7 November 2022
Available online 23 November 2022

considers the coupling effect of all targets in the bridge waterways. In addition, it is more convenient for future collision avoidance decision-making research.

The contents of the paper are arranged as follows: Section 2 presents a brief literature review concerning ship-bridge collision analysis and collision candidate detection of bridge waterways. Section 3 introduces the model design of the research and the details of the component of the proposed collision candidate detection approach in this paper. The case study is implemented in Section 4 to verify the effectiveness of the approach. Finally, the discussion and conclusion are drawn in Section 5 and Section 6 respectively.

2. Literature review

The writer aims to focus on the development of related works in ship-bridge collision avoidance and collision candidate detection of bridge waterways. In this section, the research status and defects of the above topics will be presented by analyzing the relevant literature in recent years. With that in mind, the motivation of this paper will be put forward.

2.1. Ship-bridge collision avoidance

To mitigate the damage caused by ship-bridge collisions, various methods have been proposed. Among the related literature, the methods are mainly divided into passive and active anti-collision based methods.

At present, the studies on ship-bridge collision avoidance mainly focus on passive anti-collision, which can minimize the damage caused by collision from the perspective of installing anti-collision facilities. The facilities include direct structures and indirect structures. The basic working principle of direct structures is to absorb the kinetic energy of the ship through the local plastic deformation and failure of the structure in the process of ship-bridge collision (Fan et al., 2015). More typical and commonly used are the steel fender system (Jiang and Chorzepa, 2015; Jiang and Chorzepa, 2016; Sha et al., 2019; Sha et al., 2021) and the fiber-reinforced plastic system (Fang et al., 2016; Zhu et al., 2019; Svensson, 2009). Indirect structure, as the name suggests, means that the anti-collision facilities are separate from piers, such as pile-supported structures, artificial islands, and floating protection (Chen et al., 2021; Svensson, 2009). Relatively speaking, the disadvantages of such facilities are expensive and have great impact on navigation.

Some studies focused on the active anti-collision research between ship and bridge. The studies can be divided into macro and micro active anti-collision according to different research angles (Ma et al., 2022). The macro research is to assess the probability that the bridge may collide with the ships in a certain period of time. The statistical analysis method was generally used to assess the collision probability based on the traffic flow. The standard of AASHTO. (1991), published by the American Association of State Highway and Transportation Officials, provided an approach for assessing the probability assessment of ship-bridge collision and was widely used. The standards of Larsen (1993) was proposed by the International Association for Bridge and Structural Engineering also provides an assessment approach. Besides, the Eurocode model and KUNZI model also provided the approaches for the probability assessment of collision. This kind of method can provide a reference and basis for the anti-collision decision making in the whole construction and service period.

The micro active anti-collision is a qualitative or quantitative evaluation of the ship–bridge collision risk during the period when the ship passes the bridge according to the real-time behavior characteristics of the ship and the environment, which is from the perspective of the specific ship (Ma et al., 2022). There are fewer researches on micro active anti-collision that have contributed to ship-bridge collision avoidance. Wu et al. (2019) proposed a fuzzy logic-based approach for ship-bridge collision alerts by considering ship particulars, bridge parameters, and the natural environment. Xiao et al. (2015) analyzed the AIS data in the waters of Rotterdam port and the Sutong bridge to reduce the probability of collision between ships and bridges in the future by analyzing the spatial, speed and heading distribution characteristics of traffic flow. Rutkowski (2021) summarized the marine practices and the author's research for estimating the ship's best possible speed when passing under bridges by analyzing the relationship between the overhead clearance, draft and speed. Du (2018) established a bridge anti-collision system, which mainly analyzes whether the clearance height and the clear width of bridge waters meet the navigation requirements of ships. Pedersen et al. (2020) outlined a rational design procedure for bridge piers and pylons against ship collision impacts. Liu and Xiao. (2014) proposed a collision risk model of ship-bridge based on collision avoidance theory. Both the Distance at Closest Point of Approach (DCPA) and Time to Closest Point of Approach (TCPA) are integrated into an index called the degree of collision risk.

2.2. Collision candidate detection

Various works on collision candidate detection in the field of navigation have been done in recent years. Collision candidate detection is a situation in which there is the danger of collision between ships approaching each other, but with no collision eventually occurring, either due to deceleration, or evasion by the change of course (Li et al., 2021). Collision candidate detection is of great significance for the risk analysis of maritime transportation. It gives early warnings to encountering ships by evaluating collision risk (Yoo, 2018). As for the region, the collision risk can be measured by collision candidate detection due to the number of actual collision accidents is usually very small (Shu and Yu, 2007). In general, there are two categories of methods, namely indicator-based methods, and Ship Domain (SD) based methods.

The Closest Point of Approach (CPA) is the most classical indicator-based method (Debnath and Chin, 2009; Chin and Debnath, 2009), which is still widely used in navigation practice. The collision risk exists if the DCPA is less than the safe distance and the TCPA is positive (Li et al., 2021). However, DCPA and TCPA do not fully reflect the severity level of the vessel encounter (Zhang et al., 2015). Later, the Collision Risk Index (CRI) method emerged and has been rapidly developed and applied (Mou et al., 2010, 2020; Li et al., 2019; Gil et al., 2020). It considered more indicators such as distance, bearing, and relative speed compared with the CPA method. The principle of the CRI method is to detect the collision candidate by calculating the collision risk index between own ship and the target. The output obtained by the CRI method is a value between 0 (safety) and 1 (danger) which represents the collision risk of the ship's current situation. The indicator-based methods have two shortcomings:1) It is more suitable for point obstacles and difficult to be applied to collision candidate detection of linear or other shapes obstacles; 2) Additional avoidance priority algorithm must be established in the subsequent collision avoidance decision research because there may be multiple targets with the same collision risk index.

Another research of collision candidate detection is the SD based method. The SD is the area around the ship that avoids the entrance of other obstacles for navigational safety. It was first proposed by Fujii and Tanaka (1971) in the traffic survey of Japan's coastal waters, and the domain is an ellipse, which is mainly used in narrow waters. Subsequently, Goodwin et al. (1975) and Davis (1980) respectively proposed SD models composed of three unequal sectors and off-centered circular ship domain models. Based on their work, various types of SD have been developed. According to Du et al. (2021), the SD models may be classified as probabilistic boundary SD (Zhao and Shi, 2018; Zhang and Meng, 2019), data-based SD (Hansen et al., 2013), and dynamic SD (Wang et al., 2013; Liu et al., 2016; Liu et al., 2021). There are also the following disadvantages: 1) Such methods need to detect collision candidates one by one, ignoring the coupling effect of different targets on own ship; 2) Additional avoidance priority algorithm also should be

established because own ship may enter safety domain of multiple targets at the same time.

2.3. General remarks

The above literature on ship-bridge collision analysis reveals valuable insights for bridge owners and maritime authorities to propose and implement effective risk mitigation measures. However, the previous studies focused on the ship-bridge collision mainly concentrated on passive anti-collision facilities and only a few from the perspective of active anti-collision. It can effectively reduce the damage caused by ship-bridge collision, but the probability of collision did not decrease. The role of these protective measures is very limited once the impact force exceeds the load of the facilities. Therefore, it is particularly necessary to propose an approach from the perspective of active anti-collision to reduce the collision probability of ship-bridge.

Collision candidate detection has been well developed with the aforementioned works. However, there are still some issues that compromised the accuracy and reliability of the results. The VO method (Chen et al., 2020a, 2020b), an overwhelming choice for collision candidate detection in recent years, can make up for the defects of the indicator-based methods and SD based methods. It is widely used at sea and in unrestricted waters, but it is not applied to the bridge waterways. To overcome the limitations of these previous works, this study integrated the features of the bridge waterways into the VO method to perform collision candidate detection of ship trajectories.

3. Model design

3.1. Methodology overview

For the navigation safety of ships in the bridge waterways, a data-driven approach for ship collision candidate detection of the waterway based on historical AIS data is proposed. This paper can be divided into three parts, one is the data preprocessing module, another is the feature recognition module, and the third one is the collision candidate detection module. The flowchart of the research methodology is shown in Fig. 1.

The accurate data has great significance for collision candidate detection, and the purpose of the data preprocessing module is to make the requirements of the research through decoding, outlier detection, and interpolation of the raw AIS data. The data can be decoded following the standard (ITU, 2010), and the abnormal data with obvious abnormality in longitude, latitude, Speed Over Ground (SOG), or Course Over Ground (COG) of the ships can be removed. Kinematic interpolation, a common interpolation method, will be applied between two points with large time interpolation. Through the above preprocessing, the AIS data can be used as the data basis for the following modules.

The feature recognition module aims to provide references for the collision candidate detection module by identifying the features of the bridge waterways through historical AIS data. Three features are concerned in this module: 1) The channel boundaries are identified by the KDE method based on historical ship trajectories of the waterways; 2) The basic safety domain of ships sailing in the waterways of the bridge is established, and the parameters of the domain are also identified through the KDE method and historical AIS data; 3) The safety domains of piers are formulated in combination with the anti-collision facilities of the bridge or the local navigation rules.

The third one is the collision candidate detection module based on the data preprocessing module and the feature recognition module. In this part, the basic definition of collision candidate is introduced, and the Linear Velocity Obstacle (LVO) method and Non-linear Velocity Obstacle (NLVO) method are used to perform collision candidate detection with static obstacles (channel boundary and pier) and target ships respectively.

3.2. Data pre-processing module

Referring to (ITU, 2010), the raw AIS data can be decoded and sorted by their MMSI. There are plenty of outliers and missing data in AIS data

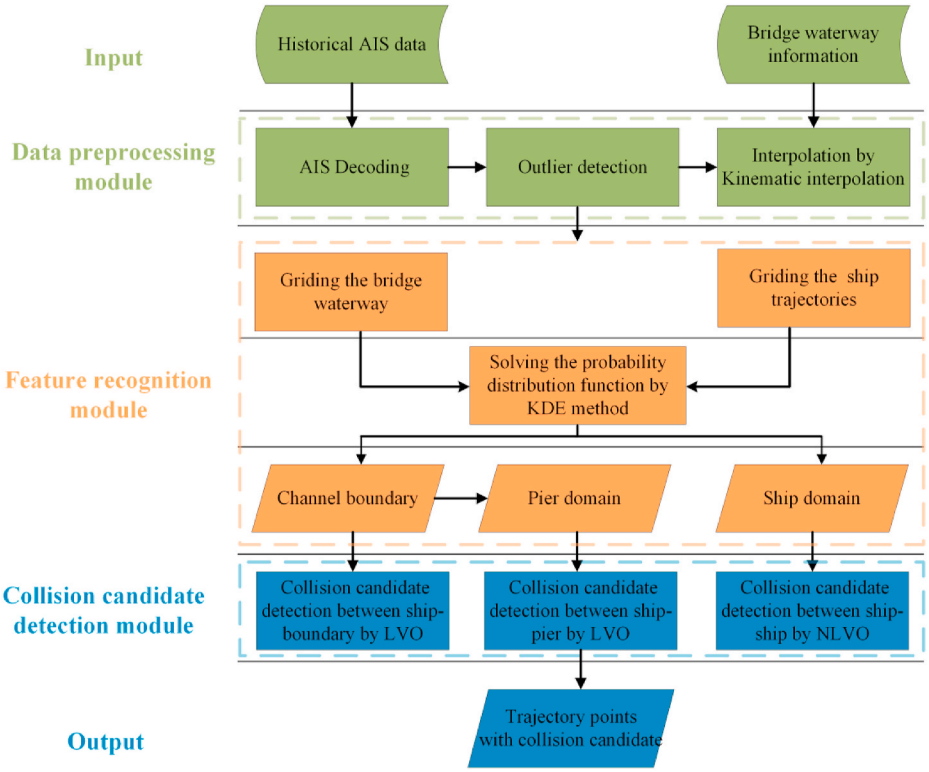

Fig. 1. Flowchart of the research methodology.

decoded, due to the AIS messages being easily affected by bad weather, blocked communication channel, equipment errors, etc. The accurate data has great significance for collision candidate detection. To acquire more precise AIS data, we will do the following processing refer to (Zhang et al., 2021(a)):

(1) Violation data, such as MMSI does not conform to the records of 9-bit, latitude, and longitude out of range, the draft is zero.
(2) Abnormal data, such as a message changes greatly/without changes in a short/long time.
(3) Overlapping data, such as the data of two adjacent trajectory points are the same except for time.

According to (ITU, 2010), the transmitting frequency of AIS data varies from 3s to 3min. Therefore, the time interval between adjacent trajectory points is inconsistent on the same trajectory. At present, the commonly used interpolation methods are linear interpolation (Xue et al., 2017), cubic spline interpolation(Zhang et al., 2018), and kinematic interpolation (Guo et al., 2021) in the field of navigation. The kinematic interpolation is used in this section, and the main idea of it is to establish an acceleration function of the moving object in a period (Guo et al., 2021). The kinematic equations are as follows:

$$\begin{cases} x(t) = x(t_i) + v(t_i)(t - t_i) + \frac{1}{2}B(t - t_i)^2 + \frac{1}{6}M(t - t_i)^3 \\ v(t) = v(t_i) + B(t - t_i) + \frac{1}{2}M(t - t_i)^2 \end{cases} \tag{1}$$

Where: $x(t)$ and $v(t)$ represent the position and velocity of the interpolated point respectively; $x(t_i)$ and $v(t_i)$ are known information of the previous point of the interpolated point. The two points before and after the interpolated point can be brought in to calculate M and B. The location and velocity of interpolated point are obtained when the time of interpolated point has been calculated, and the time is generally the average of the two points before and after.

As we know, the point of trajectory consists of time, longitude, latitude, speed, course and draft, etc. The values of time, longitude, latitude, and speed are obtained by Eq. (1) above. Normally, The draft of the same trajectory is not changed in a short time, and the course of interpolated point can be calculated as follows:

$$C(t) = \frac{(C(t_j) + C(t_i))}{2} \tag{2}$$

Where: $C(t_i)$ and $C(t_j)$ denote the course of two given adjacent points.

3.3. Feature recognition module

This section elaborates on the feature recognition module, which is to recognize the features of the bridge waterways by historical ship trajectories. The features contain channel boundary, pier domain, and ship domain, respectively. The detailed designs of the module are discussed in the following sections.

3.3.1. Recognition of channel boundary

Generally, the buoys are arranged along the channel to mark the boundaries, and to guide ships to pass safely. However, due to the limitations of various conditions (e.g. wind, current and water depth. etc.), the buoys in many bridge waterways are not fully equipped and the position changes with the change of the flow. Therefore, some great challenges and uncertainty rely on buoys to identify the channel boundary. Recently, the rapid development of AIS improves the convenience of trajectory data acquisition. The AIS data recorded the real trajectory of ships passing through the bridge waterways. These trajectories are decided by the navigator after considering various factors such as wind, current, boundary, and customary route. To sum up, it is a more accurate and reliable way to identify the channel boundary through historical AIS data.

The information related to the channel boundary is difficult to obtain from the preprocessed AIS data, as shown in Fig. 2(a). In this module, the trajectory density map is acquired by meshing the region and the trajectories shown in Fig. 2(b). Assume that the range of this region is $(x_{\min}, y_{\min})$ to $(x_{\max}, y_{\max})$ and is divided into $M \times N$ small grids. Let $T_i = \sum_{j=1}^{N} P_j$ is denote a ship trajectory with $P_j = \{x_j, y_j, c_j, v_j\}$. The index of the grid about each trajectory point can be calculated as follows:

$$\begin{cases} W_m = \left\lfloor \frac{M \cdot (x_j - x_{\min})}{x_{\max} - x_{\min}} \right\rfloor \\ H_n = N - \left\lfloor \frac{N \cdot (y_j - y_{\min})}{y_{\max} - y_{\min}} \right\rfloor \end{cases} \tag{3}$$

Where: W_n and H_n denote the index of the grid where the trajectory point P_j is located.

To accurately extract the channel boundary from the trajectory density map, a method to describe the distribution of trajectory points is necessary. The KDE method is a widely used and very suitable nonparametric estimation algorithm. Compared with traditional statistical methods, the advantage of KDE is that the fitted curve is continuous. The KDE can study the spatial distribution characteristics of AIS data directly according to the position information of the trajectory distribution (Lu et al., 2020). The equation of KDE can be expressed as:

$$\widehat{f}_h(x) = \frac{1}{n}\sum_{i=1}^{n} K_h(x - x_i) = \frac{1}{nh}\sum_{i=1}^{n} K\left(\frac{x - x_i}{h}\right) \tag{4}$$

Where: x_i represent independently distributed trajectory points; h is a smoothing parameter called bandwidth; $K(x)$ is the kernel function, including Uniform, Triangular, Gaussian, and Normal, etc. The Gaussian distribution is the most common probability distribution, and many continuous random variables encountered in real life conform to the Gaussian distribution, including the trajectory density distribution of the bridge waterways. Therefore, the Gaussian kernel is selected as the kernel function of the KDE method in this paper. The Gaussian kernel is as follows:

$$K(x) = \frac{1}{\sqrt{2\pi}} e^{\left(-\frac{x^2}{2}\right)} \tag{5}$$

Each small grid in the trajectory density map corresponds to a gray value, which is the number of trajectory points falling on the grid. As shown in Fig. 3, take out the gray value of each column and fit it with the KDE method. As the bridge waterway has an upstream channel and a downstream channel, the fitting curve has two local maximums and one local minimum, which represent the center point of the channels and the separation point between channels respectively. Taking the local minimum as the probability value of the channel boundary, the boundary points can be obtained.

After iteratively calculating the gray value of the trajectory density map by the KDE method, two boundary lines and one segmentation line composed of boundary points and segmentation points are identified, as shown in Fig. 4(a). However, the curves are not smooth and do not conform to the navigation practice. The polynomial fitting can be used to deal with the curves, and the pseudocode of polynomial fitting is shown in Table 1. T is the candidate curve that will be processed, p0 is the initial value of the fitting function, and function leastsq(error, p0, args=(x, y)) is a fitting module in Python. The final boundary lines and the separation line can be obtained after processing, as shown in Fig. 4 (b).

3.3.2. Recognition of ship domain

The research in the ship domain has a long history, and various domains for different scenarios have been put forward one after another.

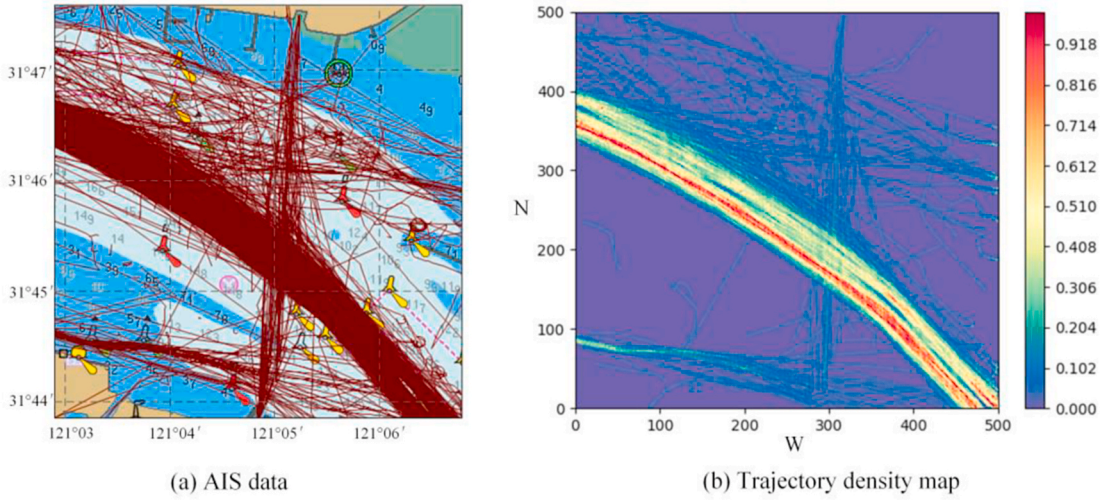

Fig. 2. AIS data and trajectory density map.

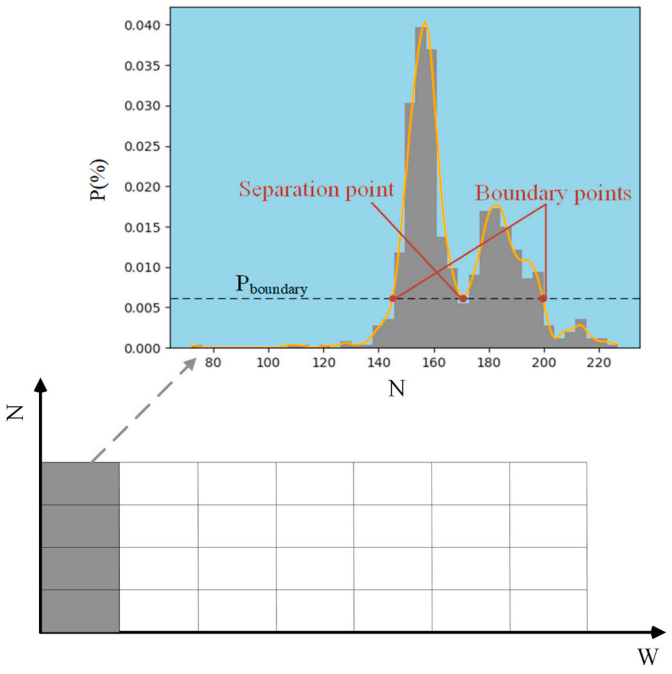

Fig. 3. Fitting of the trajectory density map by KDE.

Among them, the ship domain with the eccentric ellipse is very popular due to the consistency with navigation practice. However, the parameters of the domain are difficult to determine. The common practice for determining the parameters is to take a multiple of the ship's length, which is not interpretable and varies with the navigation environment in the water area. In this paper, the parameters which more suitable for the selected region are determined by the KDE method which is based on historical AIS data.

To simplify the model, the ship is regarded as a particle and the center of the ship (x_i, y_i) is used instead of the position. As shown in Fig. 5(a), the parameters that determine the ship domain are the long and short semi-axes (a, b) and the coordinate of the virtual ship $P_i^{'}(x_i^{'}, y_i^{'})$. In previous studies, the parameters are mostly set by experience and do not provide an interpretable method to solute them. In this paper, the ships of the same characteristics are classified into one class. Suppose P_i is the trajectory point of the detected ship and P_j is the point of another ship around it. The distance and relative bearing of the two ships are expressed as $d(P_i, P_j)$ and $rb(P_i, P_j)$. The trajectory points of other ships can divide into different regions according to relative bearing as shown in Fig. 6(a).

As shown in Fig. 6(b), the fitting curve of the distance of each region can be obtained by the KDE method (Mentioned in Section 3.3.1). By setting the threshold of probability in the range of 0–1, the distance parameter of each region can be obtained as follows:

$$\alpha = \int_{D_{\min}}^{D} f(x)dx \tag{6}$$

Where: α is the threshold of probability; $D_{\min}$ is the minimum distance between the detected ship and other ships; $f(x)$ is the fitting curve by the KDE method; D is the distance parameter of the region.

As shown in Fig. 5(b), assuming that a_1, a_2, b_1, b_2 represent the distance parameters of four regions respectively. The parameters of the ship domain can be determined by the follows:

$$\begin{cases} x_i^{'} = x_i + \dfrac{(b_2 - b_1)}{2} \\ y_i^{'} = y_i + \dfrac{(a_1 - a_2)}{2} \\ a = \dfrac{a_1 + a_2}{2} \\ b = \dfrac{b_1 + b_2}{2} \end{cases} \tag{7}$$

Where: (x_i, y_i) and $(x_i^{'}, y_i^{'})$ are the position of the real ship and virtual ship; a and$b$ are long and short semi-axes of ship domain with the eccentric ellipse.

Assume α is the true course of the detected ship, the expression of the ship domain with the eccentric ellipse is as follows:

$$\frac{\left((x - x_i^{'})\cos\alpha + (y - y_i^{'})\sin\alpha\right)^2}{a^2} + \frac{\left((x - x_i^{'})\sin\alpha - (y - y_i^{'})\cos\alpha\right)^2}{b^2} = 1 \tag{8}$$

3.3.3. Recognition of pier domain

The collision between ships and piers may pose the biggest threat to the bridge. Plenty of research focuses on making the pier stronger, and a few concentrate on preventing ships from colliding with piers. In this paper, a collision between them is avoided by delimiting the safety domain for piers. The pier domain can be determined in many ways. This section mainly introduces how to determine the domain through the existing anti-collision facilities or historical AIS data.

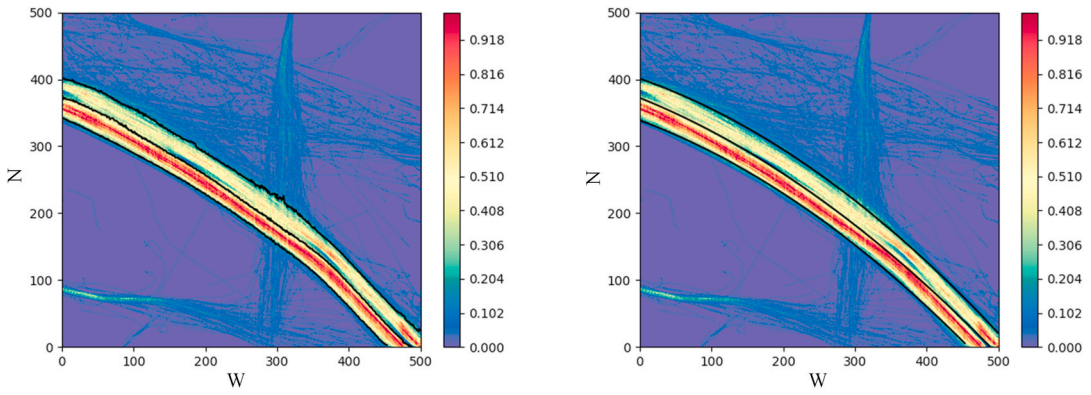

(a). Channel boundaries obtained by KDE (b). Channel boundaries dealt by polynomial fitting

Fig. 4. Channel boundaries identified from AIS data.

Table 1
The pseudocode of polynomial fitting.

Algorithm of polynomial fitting: Fitting(T)	
1	x = T["x"]; y = T["y"]
2	p0 = [a1, a2, a3]
3	error = a1*x^2 + a2*x + a3-y
4	para = leastsq(error, p0, args=(x, y))
5	a1, a2, a3 = para
6	y_fitted = a1*x^2 + a2*x + a3
7	return x, y_fitted

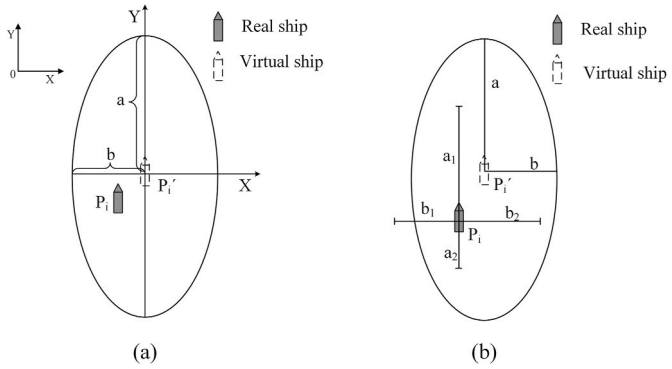

Fig. 5. The ship domain with the eccentric ellipse.

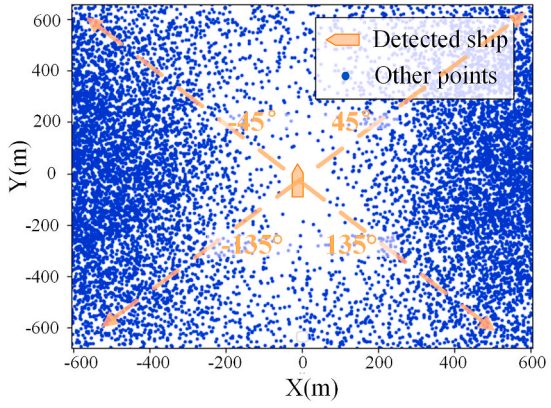

(a). Trajectory points divide by relative bearing

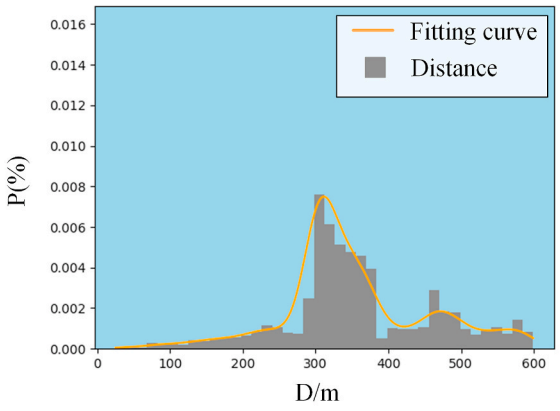

(b). Fitting curve of a region by KDE method

Fig. 6. Trajectory points around the ship to be detected.

Generally, the anti-collision facilities should be set for bridge safety. The distance between facilities and piers has been strictly demonstrated to meet the standards and local channel conditions before setting. Therefore, the distance can be used as a reference for setting up the pier domain. As shown in Fig. 7, the rectangles are regarded as safety domains of the piers, because there are anti-collision facilities on both sides of the piers. The length and width of the area are determined by the distance between the pier and the anti-collision facilities and the distance between the pier and the channel boundary.

3.4. Collision candidate detection module

To provide a reliable and understandable approach to detecting the collision risk of historical ship trajectories in bridge waterways. A collision candidate detection approach, considering multiple risk factors in the process of a ship crossing the bridge, is designed in this section. Generally, a collision candidate is defined as the ship and target in an encounter process where their spatio-temporal relationships satisfy certain criteria that has the potential for collision (Chen et al., 2018). Therefore, a collision candidate exists when the following basic equation is satisfied.

$$P_i(t_f) \in P_t(t_f) \oplus SD\left[P_t(t_f)\right] \tag{9}$$

Where: $P_i(t_f)$ and $P_t(t_f)$ represent trajectory points to be detected and target at the time t_f, respectively; SD is the safety domain of target.

When a ship is sailing in the bridge waterway, the safer practice is to follow the channel at a safe speed. In this process, the channel boundary

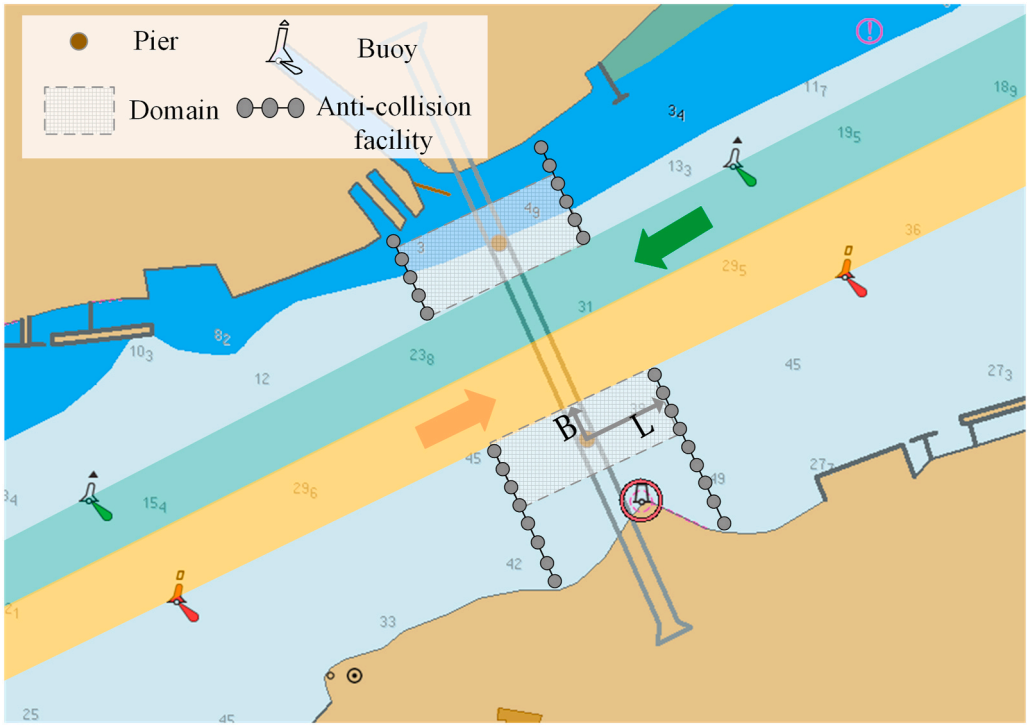

Fig. 7. Safety domain of pier.

and pier can be regarded as static obstacles, which linear motion with a velocity of 0. The target ship is a dynamic obstacle with nonlinear motion. The following sections will introduce the collision candidate detection between ship trajectory and static or dynamic obstacles in sections 3.4.1 and 3.4.2. To describe this process more vividly, examples are shown respectively.

3.4.1. Collision candidate detection with static obstacle

In section 3.3.1, the channel boundaries, composed of multiple points, were recognized from historical AIS data. Assume that $L = \sum_{t=1}^{N} P_t$ denote a channel boundary with $P_t = \{x_t, y_t\}$. Because the boundary can be regarded as a static obstacle with an infinitesimal safety domain. Eq. (9) can be substituted with Eq. (10):

$$P_i(t_f) \in \sum_{t=1}^{N} P_t(t_f) \tag{10}$$

Considering the assumption that the detected ship will remain in current motion and the motion of the boundary is linear, Eq. (10) can be substituted with Eq. (13):

$$P_i(t_f) = P_i(t_0) + \vec{V}_i(t_f - t_0) \tag{11}$$

$$\sum_{t=1}^{N} P_t(t_f) = \sum_{t=1}^{N} P_t(t_0) \tag{12}$$

$$\vec{V}_i \in \frac{\sum_{t=1}^{N} P_t(t_0) - P_i(t_0)}{t_f - t_0} \tag{13}$$

Eq (13) is the collision candidate detection equation between trajectory point and channel boundary. Let $P_t = \{x_t, y_t\}$ is the center of a pier. Eq. (9) can be substituted with Eq. (15) due to the motion of the pier being linear.

$$P_t(t_f) = P_t(t_0) \tag{14}$$

$$P_i(t_f) \in P_t(t_0) \oplus SD[P_t(t_0)] \tag{15}$$

A collision candidate between the trajectory point and pier occurs as the following condition is satisfied:

$$\vec{V}_i \in \left(\frac{P_t(t_0) - P_i(t_0)}{t_f - t_0}\right) \oplus \frac{SD[P_t(t_0)]}{t_f - t_0} \tag{16}$$

To describe the process of collision candidate detection more vividly, examples are shown respectively. As shown in Fig. 8(a), it exhibits a ship trajectory composed of four points and two border boundaries. The boundaries can be projected into the velocity space of each trajectory point using Eq. (13). Through the velocity space, it is easy to judge the collision candidate between trajectory points and boundaries. A trajectory and two piers with rectangular safety domains are shown in Fig. 8 (b). As same with above, Eq. (16) is used to project the piers into the velocity space of trajectory points.

The velocity spaces corresponding to the 1st and 2nd trajectory points of Fig. 8(a) were shown in Fig. 9. The green and red areas are the two boundaries projected to the velocity space respectively, and the black arrows represent the velocity of the trajectory points to be detected; The circle marked as a dotted line represents the maximum velocity of the ship. A collision candidate occurs when the arrow points beyond the areas, such as in Fig. 9(b). Different from them, it means the trajectory point is safe when the arrow is located between the areas as shown in Fig. 9(a).

Fig. 10 are the velocity spaces of the 1st and 3rd points in Fig. 8(b) respectively. The green and red areas in the figures correspond to the two pier domains at time t_0 to t_f. It can be seen that in Fig. 10(b), the velocity falls within the projection of the green area, which means that this point is a collision candidate point. Another point has no collision candidate risk with the piers because the velocity does not fall in the areas projected by the piers.

3.4.2. Collision candidate detection with dynamic target

In general, the ship trajectory is non-linear and deterministic. The trajectory of non-linear motion can also be projected to the velocity space of the point to be detected, but the premise is that the motion of the point is linear. Assume that $T_i = \sum_{i=1}^{N} P_i$ and $T_j = \sum_{i=j}^{N} P_j$ are the

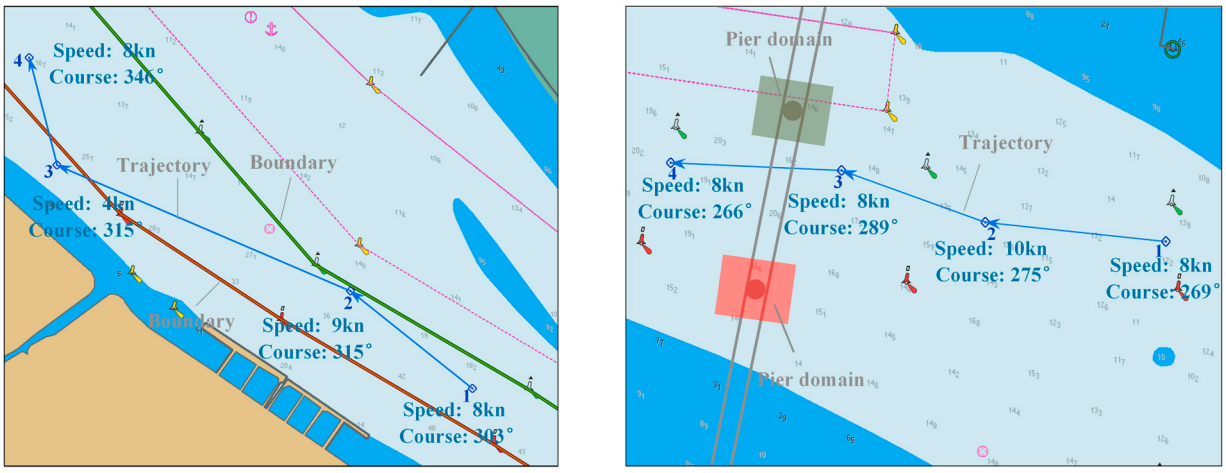

(a). The diagram of boundaries and trajectory (b). The diagram of pier domains and trajectory

Fig. 8. Collision candidate detection between trajectory and static obstacles.

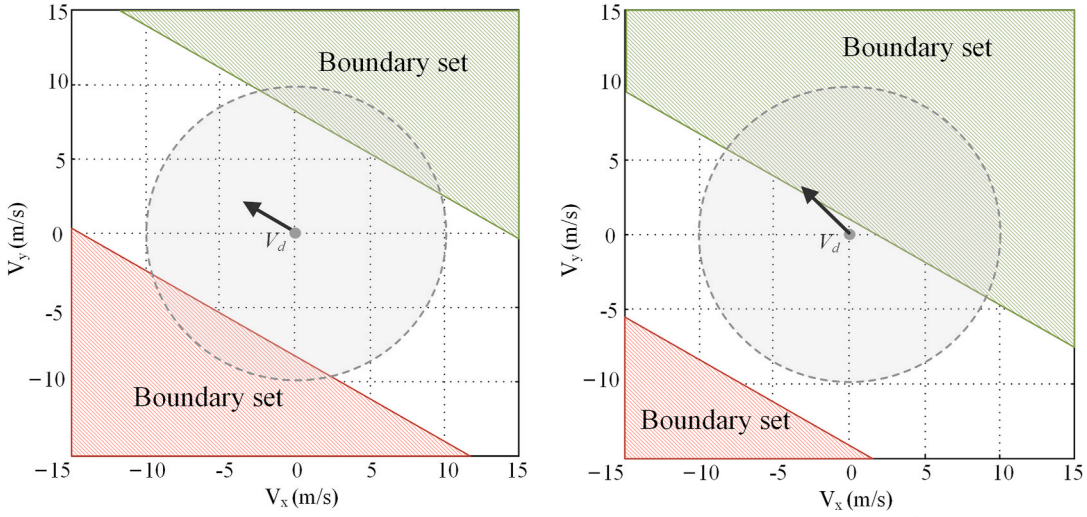

(a) Velocity space of the 1st trajectory point (b) Velocity space of the 2rd trajectory point

Fig. 9. Velocity space of trajectory points with channel boundaries.

trajectories to be detected and a nearby ship trajectory respectively. The NLVO method is used to detect the collision candidate between the two trajectories. Assume P_i is the point of detected trajectory at the time t_0, and the detection duration is t_s seconds. The trajectory of another ship only needs to retain the clip of trajectory with $T_j = \sum_{j=t_0}^{t_0+t_s} P_j$. The equation of collision candidate detection between P_i and $T_j = \sum_{j=t_0}^{t_0+t_s} P_j$ is as follows:

$$\overrightarrow{V}_i \in \sum_{t_f=t_0}^{t_0+t_s} \left(\frac{P_j(t_f) - P_i}{t_f - t_0} \oplus \frac{SD[P_j(t_f)]}{t_f - t_0} \right) \tag{17}$$

An example is used to display the process of collision candidate detection as shown in Fig. 11. Among them, the blue line is the trajectory to be detected, and the other lines are trajectories of target ships. After projecting the trajectories into the velocity space of the detected trajectory using Eq. (17), potential collision risk occurs as the velocity of the detected falls in the projected areas of other trajectories. As shown in Fig. 12(a), the first point of the detected trajectory is not a collision candidate point because the velocity does not fall in the projected areas. The velocity of the 3rd point falls in the red area as shown in Fig. 12(b), which means that the point has a potential collision risk with one of the target ships.

4. Case study

4.1. Case design

To demonstrate the effectiveness of the proposed method, the case study on collision candidate detection is illustrated in this section. Sutong Bridge, one of the busiest bridges on the Yangtze River, is located between Nantong and Suzhou (Changshu) in the east of Jiangsu Province. The channels of the Sutong bridge are divided into deep water (for ships more than 80 m) and recommended water (for ships less than 80 m) according to *The regulations on the ship routing system in the Jiangsu section of the Yangtze River (2013)*. As shown in Fig. 13, the blue and yellow channels are the deep water and the recommended water respectively. Generally, the bridge has several piers, this case only focuses on two piers on both sides of the main navigation hole, because most ships navigate through the hole. The coordinates of the two piers are (120.9958°E, 31.7824°N) and (120.9939°E, 31.7728°N) respectively.

A total of 3098 historical ship trajectories records from the area in

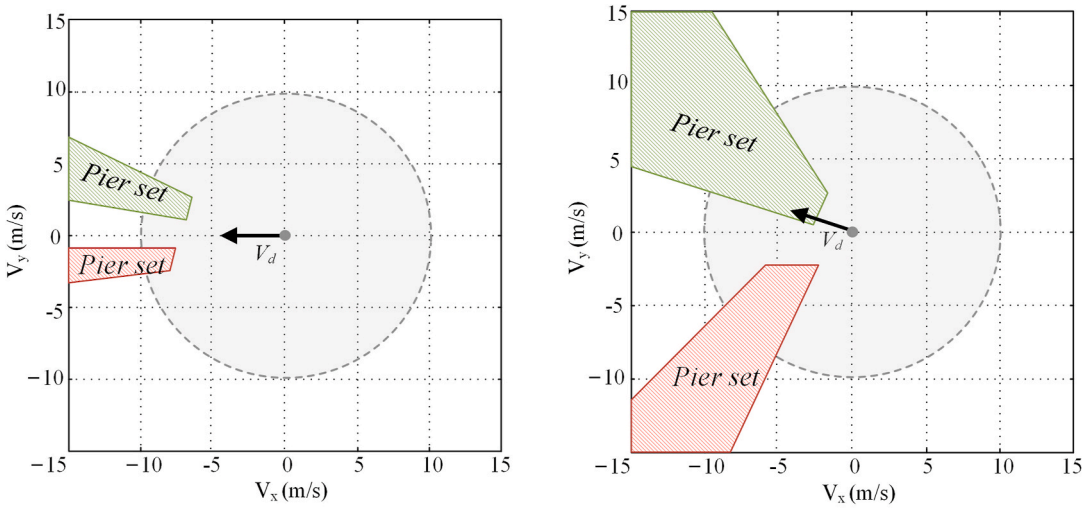

(a) Velocity space of the 1st trajectory point (b) Velocity space of the 3rd trajectory point

Fig. 10. Velocity space of trajectory points with piers.

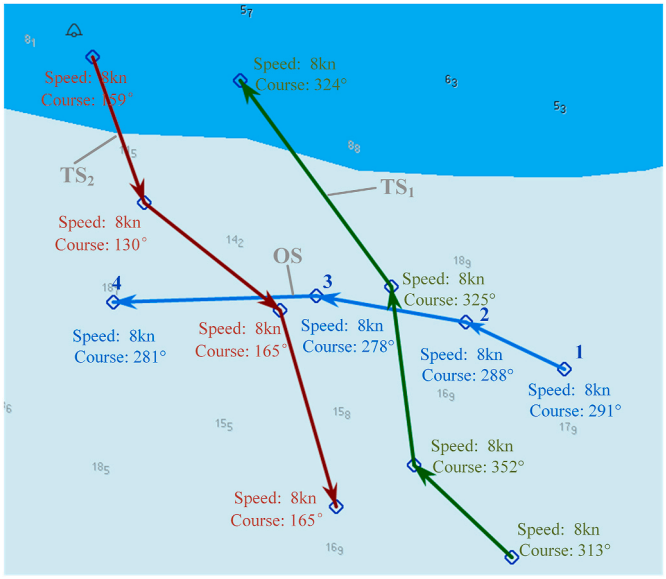

Fig. 11. The diagram of the trajectory to be detected and target ships.

the week of March. 1, 2019 to March. 7, 2019, which are used for feature recognition. Among collected data, 6 ship trajectories were selected for collision candidate detection. The details of selected trajectories are shown in Table 2.

For the convenience of calculation, the longitude and latitude are converted into WGS84 coordinates using the following equation. The value of C is 20037508.34, which is the circumference of the earth.

$$\begin{cases} x = lon \cdot \dfrac{C}{360} \\ y = \log\left(\tan\left(\dfrac{(90 + lat)\cdot\pi}{360}\right)\right) \cdot \dfrac{C}{2\pi} \end{cases} \tag{18}$$

4.2. Result of feature recognition

In this section, the features of the Sutong bridge will be identified by the methods described in Section 3.3 based on the collected historical trajectories. The experimental parameters and results will be described and displayed in detail.

4.2.1. Result of channel boundary

The collected ship trajectories are shown in Fig. 14(a) after data decoding, cleaning, and interpolation. The waterway selected is divided into 500 × 500 small grids in this study. The index of the small grid corresponding to each trajectory point can be calculated by Eq. (3). The gray value of each small grid is obtained after all indexes are counted, and the trajectory density map of the waterway is shown in Fig. 14(b). Two trajectories zones with higher density in Fig. 14(b) are deep water channels, and the ones with relatively low density on both sides are recommended channels. The KDE method will be used to identify the channel boundary in the next step based on the density map.

The KDE method can be used for preliminary boundary identification after obtaining the trajectory density map. Randomly extract four columns of data in the density map, such as 21, 214, 346, and 478. Substitute them into the KDE method with the bandwidth of 2 and Gaussian kernel respectively. The fitting curves corresponding to every column of data are shown in Fig. 15. The horizontal axis and vertical axis represent the line number and the corresponding probability distribution respectively.

The fitting curve of each column of data has four obvious convex parts in Fig. 15, of which the two in the middle represent deep water channels and the two sides represent recommended channels. There are three minimum points (P_2, P_3, and P_4) between channels in each fitting curve, among which P_3 corresponds to the boundary point between two deep-water channels, and P_1 and P_2 are the boundary points between the deep water channel and the recommended channel. The boundary points P_1 and P_5 on the outside of the recommended channel can be solved by the probability corresponding to P_1 and P_2. Through the above steps, the five separation points of each column of data are solved. As shown in Fig. 16(a), five boundary lines of the Sutong bridge can be preliminarily identified after iterating each column of data according to the above steps. Finally, the smooth boundaries can be obtained by polynomial fitting as shown in Fig. 16(b).

4.2.2. Result of ship domain and pier domain

To study the domains of different types of ships in the Sutong bridge, the ships are divided into four categories according to the length (80 m) and the average heading (180°). The results of the classification are shown in Table 3. Take the ship to be detected as the center and divide the surrounding area into four regions according to 45° and 135° of port and starboard. The distance and relative bearing between similar ships and other ships can be obtained by the method described in 3.3.2. According to the relative bearing, other ship trajectory points can be

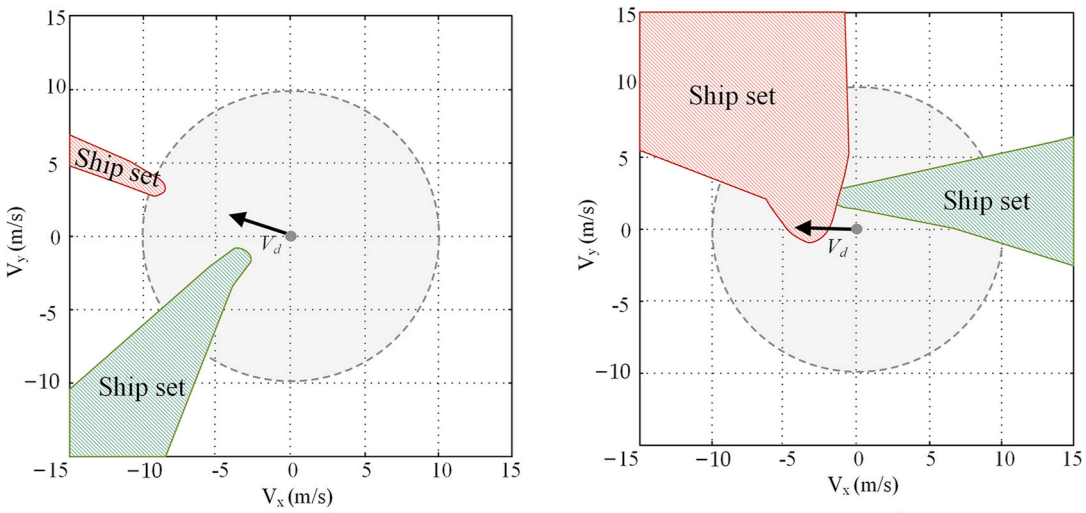

(a) Velocity space of the 1st trajectory point (b) Velocity space of the 3rd trajectory point

Fig. 12. Velocity space of trajectory points with ships.

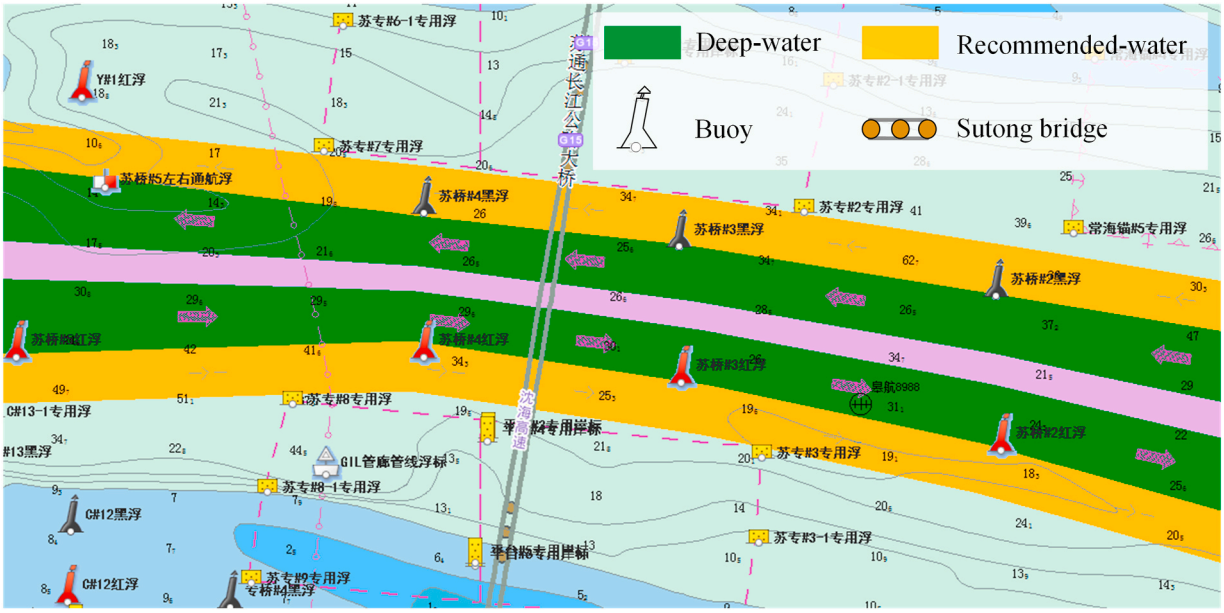

Fig. 13. The channels of the Sutong bridge.

Table 2
The information of the selected trajectories.

MMSI	Type	Length (m)	Draft (m)	Time begins	Time end
413 XXX 440	Tanker	104	6.5	March 01, 04:09:49	March 01, 04:20:00
413 XXX 656	Cargo	50	3.0	March 02, 03:13:01	March 02, 03:30:34
413 XXX 231	Cargo	64	3.0	March 02, 10:19:32	March 02, 10:42:32
413 XXX 110	High-speed craft	33	3.5	March 02, 12:36:45	March 02, 12:58:34
353 XXX 000	Cargo	89	5.3	March 02, 01:13:12	March 02, 01:26:53
412 XXX 050	Cargo	85	5.0	March 02, 01:11:30	March 02, 01:25:39

divided into different regions.

Fig. 17 shows the fitting curve of four types of ships respectively. The horizontal axis is the distance and the vertical axis is the probability distribution. The yellow solid lines and dotted lines are the fitting curves of the front and behind regions, while the blue represents the two sides regions. In this study, 1/3 of the maximum probability of the fitting curve is taken as the probability threshold. The distances corresponding to points a_1, a_2, a_3 and a_4 in the figures are the indexes for calculating the parameters of the eccentric elliptical domain of each type of ship. The domain parameters can be identified by Eq (7), and the results are shown in Table 4. The a and b in the table represent the long and short semi-axes of the ship domain respectively. And the Δx and Δy represent the distance between the virtual ship and the real ship.

The rectangles are regarded as safety domains of the two piers. In this paper, the length and width of the rectangular are determined to be 900 m and 500 m respectively by measuring the distance between the pier and the identified channel boundary, and the distance between the pier and the anti-collision facilities.

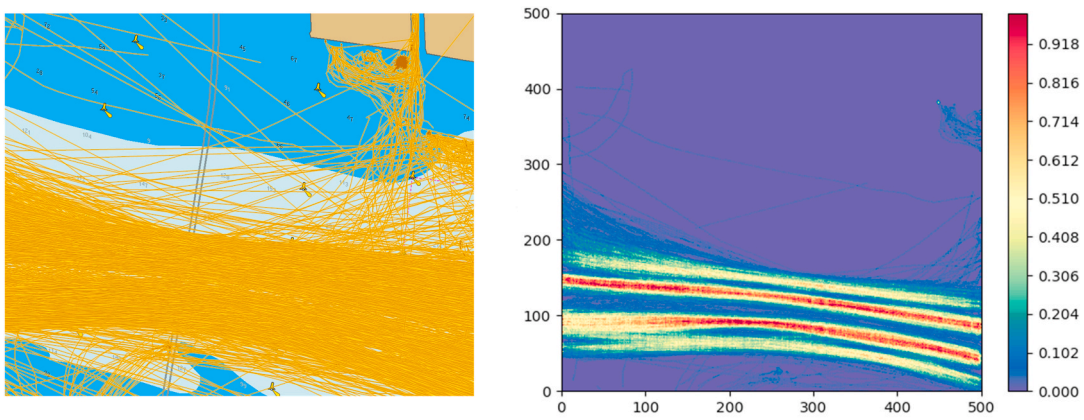

Fig. 14. The trajectories of the Sutong bridge waterway.

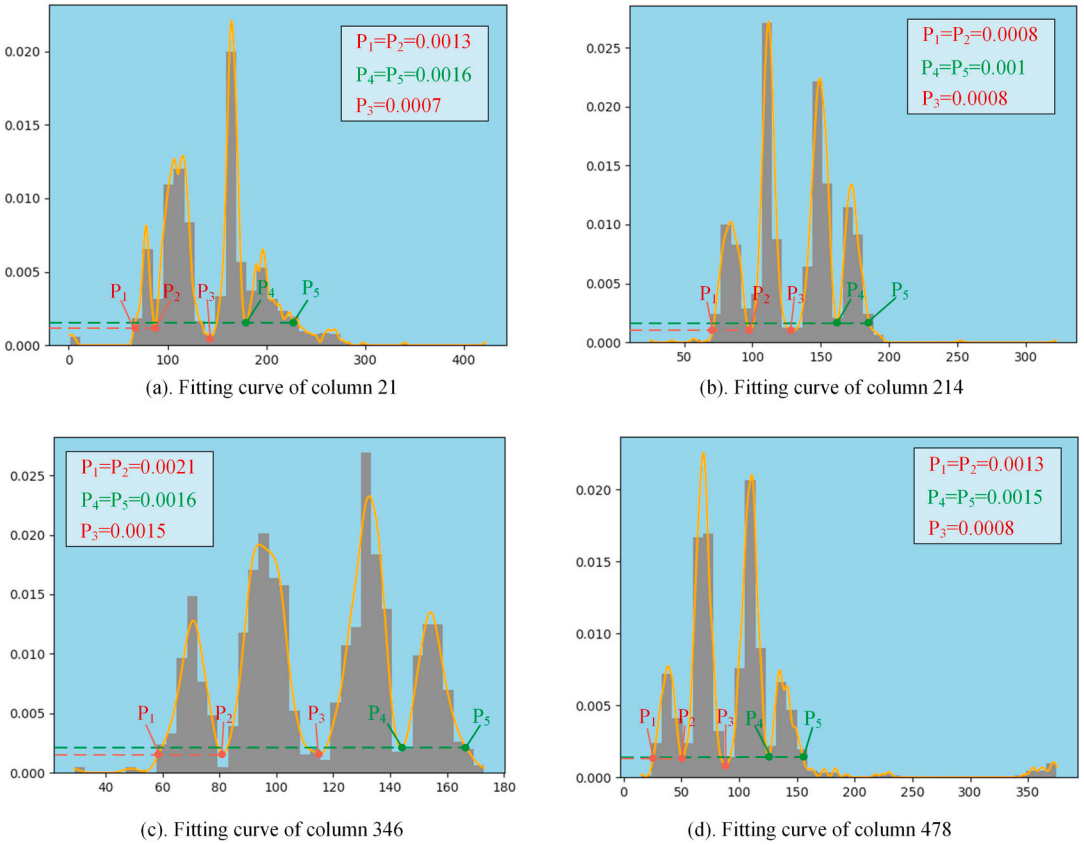

Fig. 15. Fitting curves of randomly selected columns by the KDE method.

4.3. Result of collision candidate detection

A collision candidate detection approach between ships to be detected and static or dynamic obstacles in bridge waterway was introduced in section 3.4. In this section, 6 trajectories are selected to perform and demonstrate the performance of the proposed approach. As shown in Fig. 18, the yellow and green short dashed lines represent the recommended and deep water boundaries of the Sutong bridge respectively. The area between the two deepwater boundaries is a separation zone, separating the upstream and downstream channels. The blue dots with arrows represent the trajectories to be detected.

The process of collision candidate detection between the 1st, 9th, 11th, and 13th trajectory points of the ship 353XXX000 and channel boundaries, piers, and other ships are shown in Figs. 19–21 respectively. The detection time is set to 100 s. Fig. 19 shows the detection results of the points and the channel boundaries, in which the red and blue lines are the projections of the channel boundaries on both sides of the ship to be detected. The velocities of the 1st and 9th trajectory points in Fig. 19 (a) and (b) are between the projections of the boundaries, which show that the points are safe within the detection time. In Fig. 19(c), the velocity is located in the projection area of the upper boundary, which means that the ship will leave the channel within the detection time, so the 11th point is considered to be a candidate point for collision with the channel boundary. Fig. 19(d) shows that the ship has sailed out of the

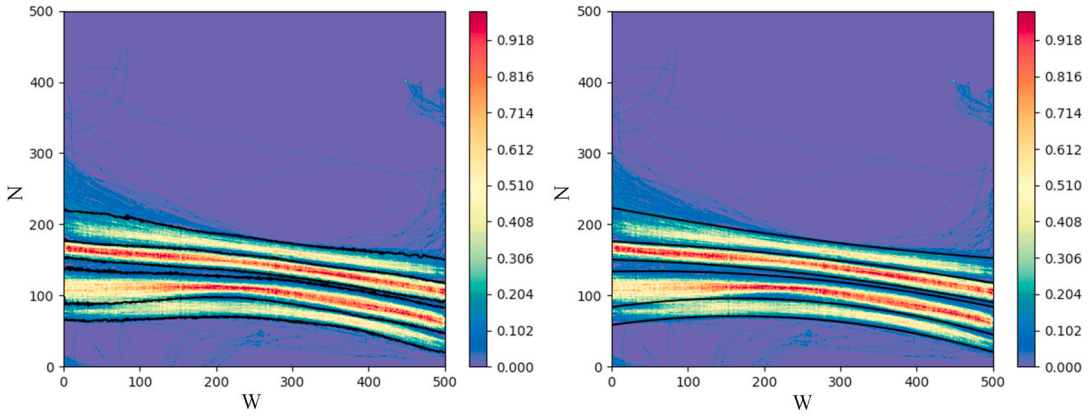

(a). Boundaries identified by KDE (b). Boundaries fitted by Polynomial

Fig. 16. Boundaries are identified by the KDE method and polynomial fitting.

Table 3
The results of the classification.

Course	Length	Number	Proportion	Type
≥180°	≥80 m	1052	34%	Type 1
	<80 m	452	14.6%	Type 2
<180°	≥80 m	1054	34%	Type 3
	<80 m	540	17.4%	Type 4

Table 4
Domain parameters for each type of ship.

Type	a (m)	b (m)	Δx (m)	Δy (m)
Type 1	206	168	−6	+8
Type 2	122	90	+8	+9.5
Type 3	213	167	+5	+8
Type 4	138	96	+10	+8

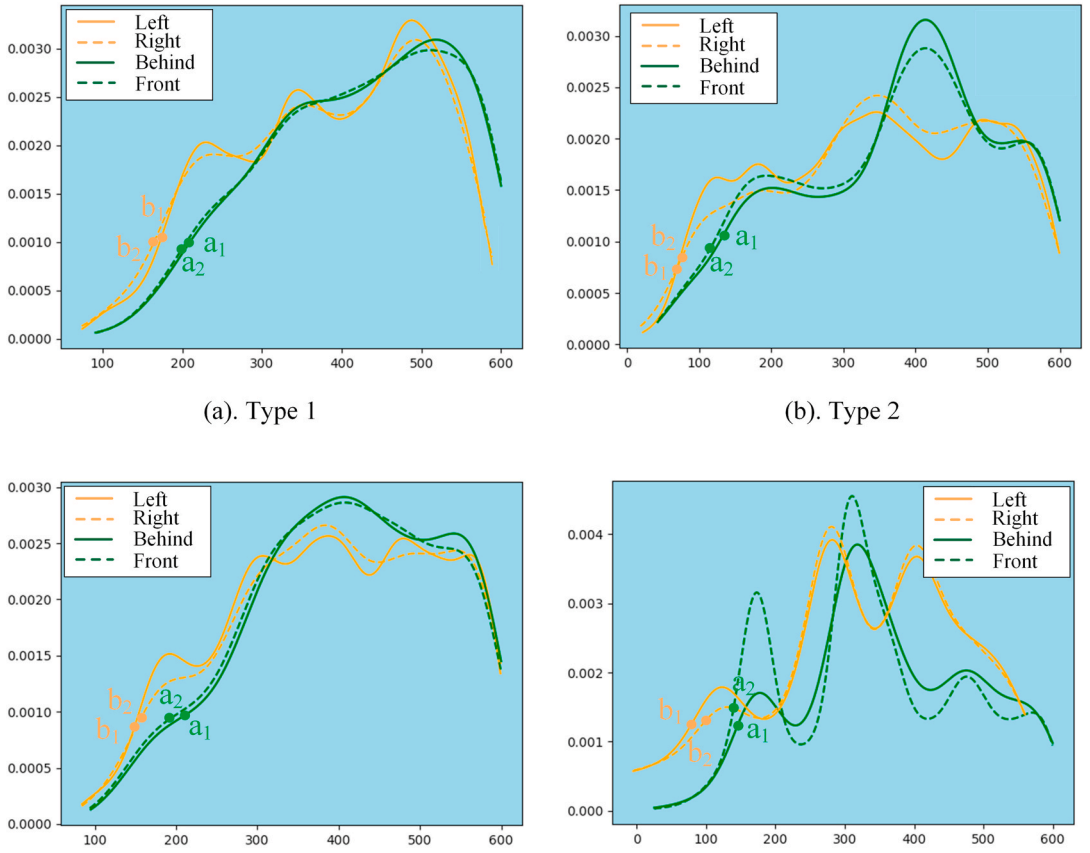

(a). Type 1 (b). Type 2

(c). Type 3 (d). Type 4

Fig. 17. The curves of distance distribution by the KDE method.

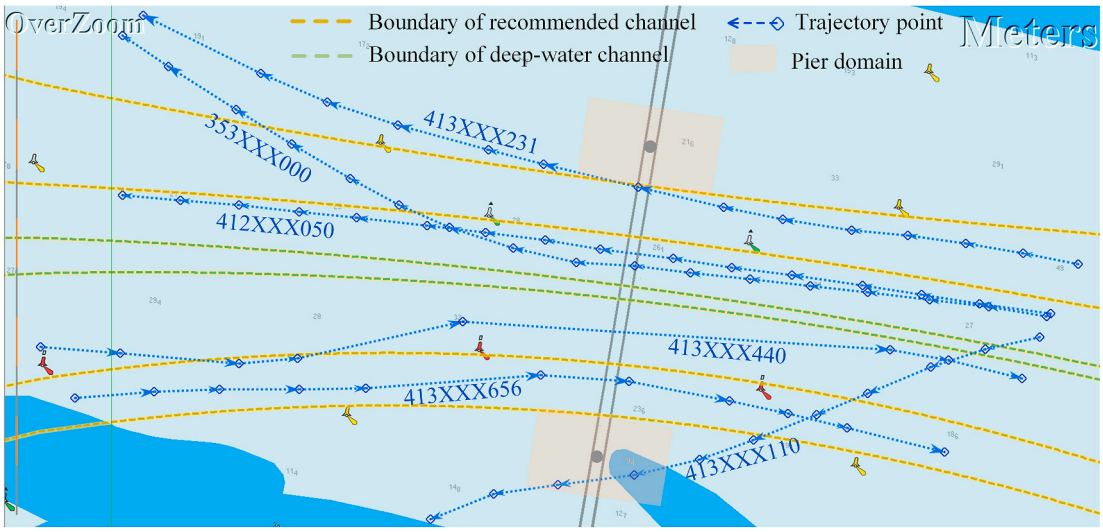

Fig. 18. Trajectories to be detected.

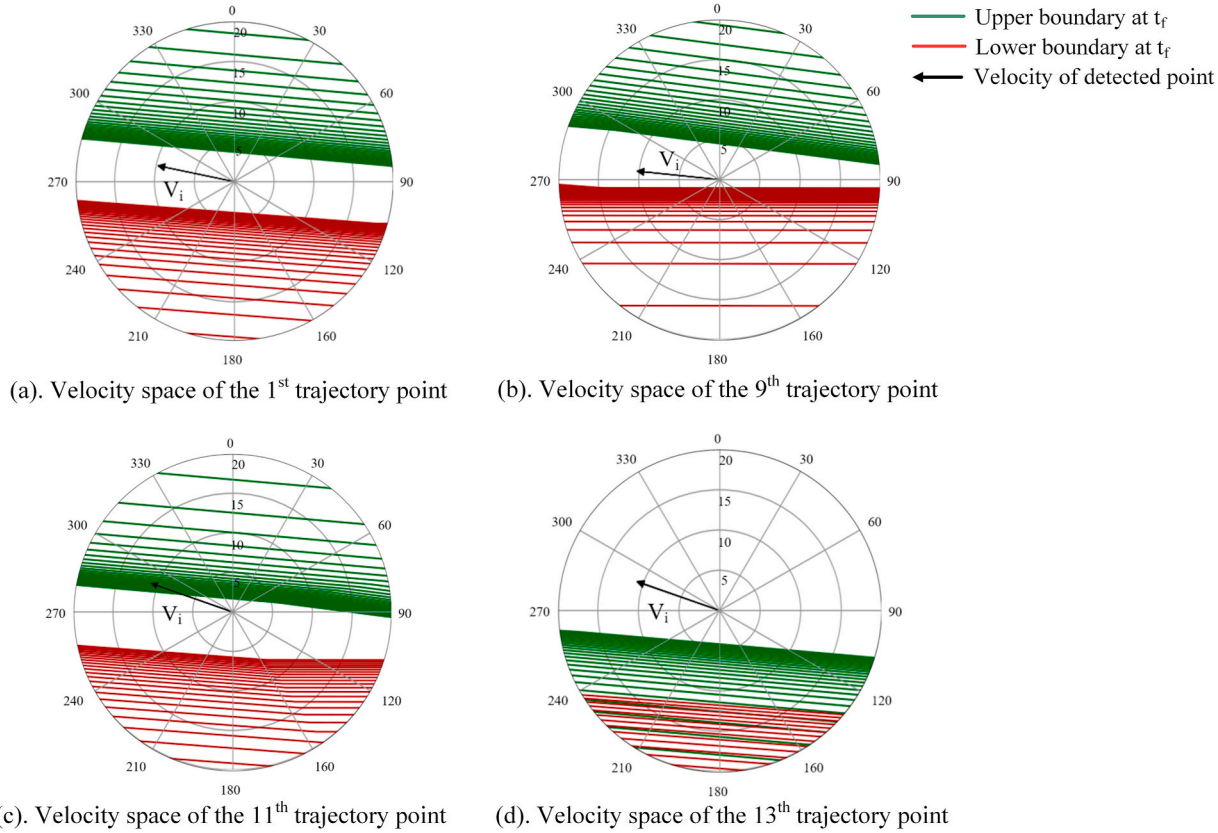

(a). Velocity space of the 1st trajectory point (b). Velocity space of the 9th trajectory point

(c). Velocity space of the 11th trajectory point (d). Velocity space of the 13th trajectory point

Fig. 19. Velocity spaces of the ship 353XXX000 with channel boundaries.

channel, such a trajectory point is also considered a collision candidate point because it does not sail in accordance with the regulations.

Fig. 20 shows the collision candidate detection results of the 1st, 9th, 11th, and 13th trajectory points of ship 353XXX000 and the piers on both sides. The red and blue areas in the velocity spaces are the projections of the two piers. There is no risk of collision with the piers at these points because the velocities do not fall on the projection areas. Fig. 21 shows the results of collision candidate detection between these points and nearby ships. Ship 353XXX000 and 412XXX050 are overtaking situations, of which ship 353XXX000 is an overtaking ship. It can be seen from the results that the 1st, 9th and 11th points are collision candidate points, while the 13th point does not have a potential collision risk with ship 412XXX050.

Figs. 19 and 21 show the process of collision candidate detection of ship 353XXX000. Next, two groups of experiments are set at t_f equal to 30 s and 60 s to display the results of collision candidate detection for each trajectory. The results are shown in Figs. 22 and 23 the blue and red dots with arrows represent the normal and collision candidate points respectively. According to the results of the two groups of experiments, four ships are detected to have potential collision risk, namely

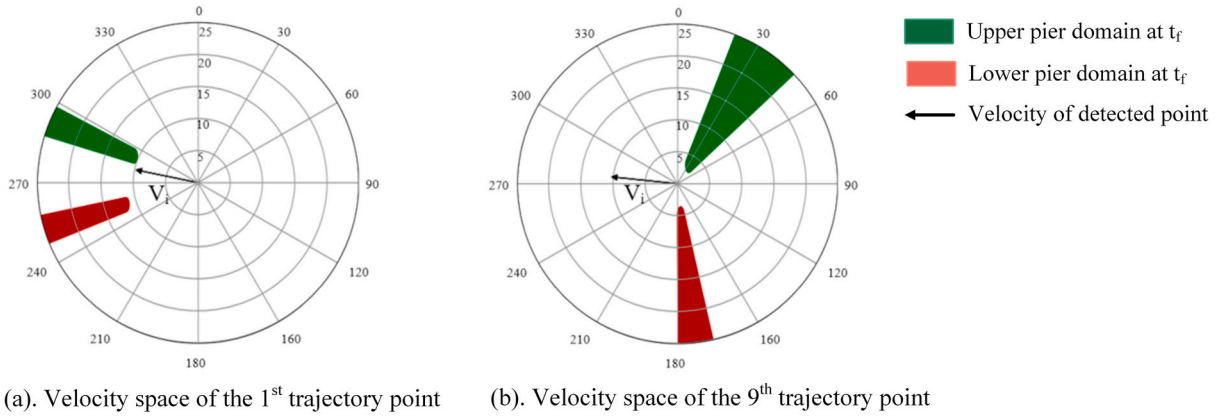

(a). Velocity space of the 1st trajectory point (b). Velocity space of the 9th trajectory point

(c). Velocity space of the 11th trajectory point (d). Velocity space of the 13th trajectory point

Fig. 20. Velocity spaces of the ship 353XXX000 with piers.

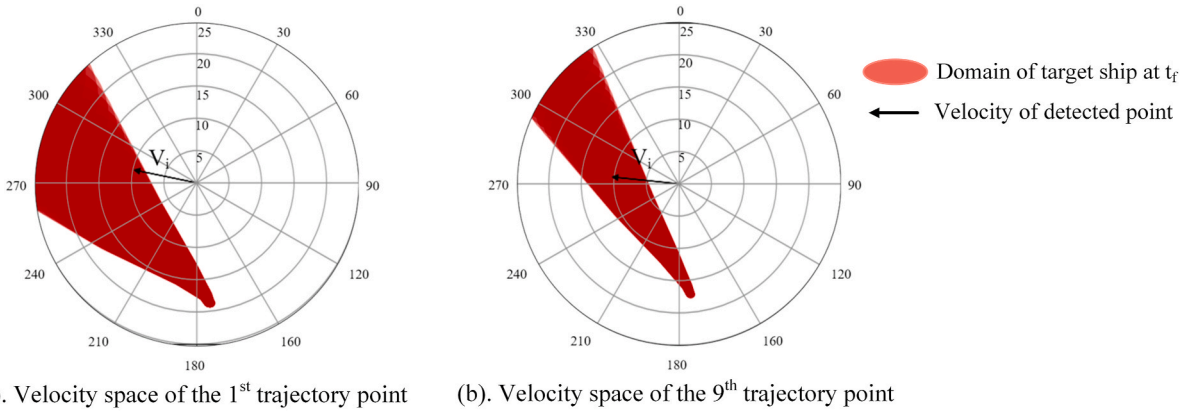

(a). Velocity space of the 1st trajectory point (b). Velocity space of the 9th trajectory point

(c). Velocity space of the 11th trajectory point (d). Velocity space of the 13th trajectory point

Fig. 21. Velocity spaces of the ship 353XXX000 with other ships.

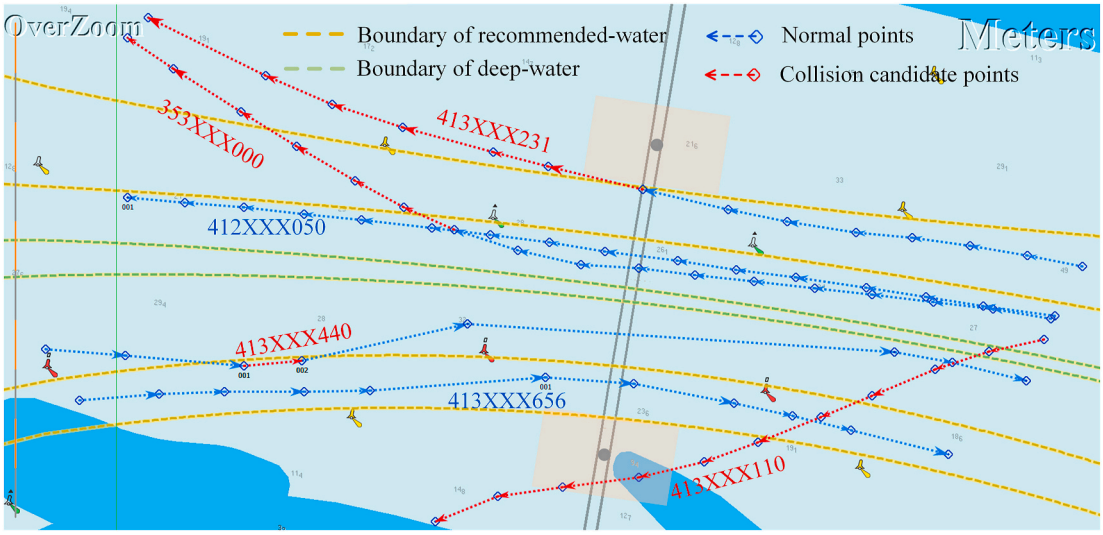

Fig. 22. Result of collision candidate detection with $t_f = 30s$

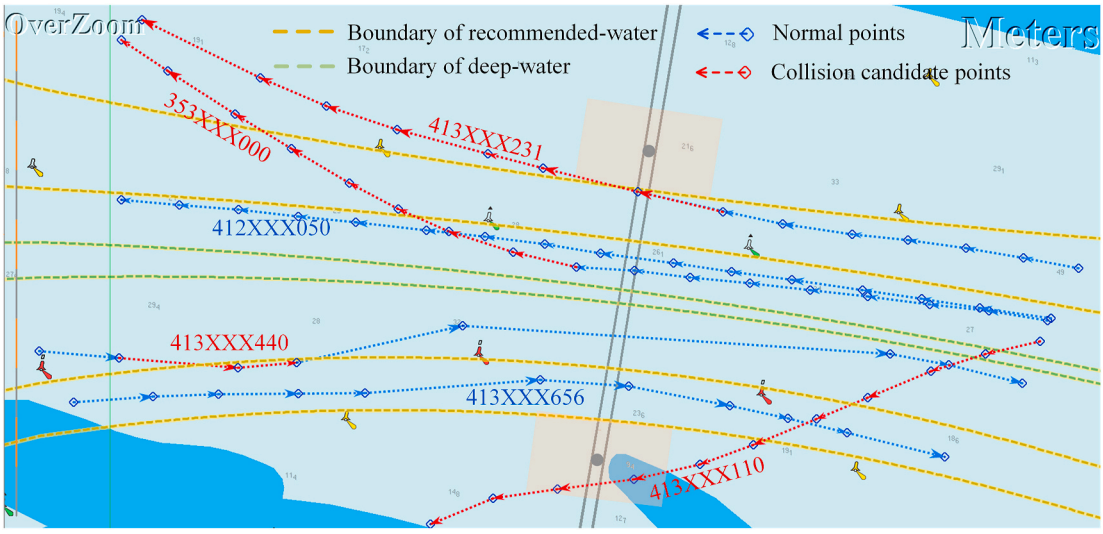

Fig. 23. Result of collision candidate detection with $t_f = 60s$

413XXX231, 353 XXX 000, 412 XXX 050, and 413 XXX 440, while ships 412 XXX 050 and 413 XXX 656 were safe. The detailed data about collision candidate detection of each ship trajectory are shown in Fig. 24.

Fig. 22 shows the results of collision candidate detection for each trajectory, the horizontal axis coordinate is the number of trajectory points, and the vertical axis coordinate is the time of collision candidate happened. Among them, the green, blue and red lines are the timelines between the trajectories to be detected and the channel boundaries, piers, and other ships, respectively. There is no collision candidate when the detection time is equal to 100s, due to the upper limit of the time being set to 100s. Figs. 23 and 24 show the detection results after setting the time threshold t_f equal to 30s and 60s, respectively. A collision candidate happened when the detection time was less than t_f. For ship 413XXX231, the results show that the trajectory points 8 to 14 are collision candidate points when t_f equal to 30s, and point 7 also is a collision candidate point if t_f is 60s. Points 1 to 11 and 10 to 17 of ship 353XXX000 have potential collision risks with other ships and boundaries respectively when t_f equal to 60s. As for ships 412XXX050 and 413XXX656, the results show that they abide by the navigation rules of the Sutong bridge.

5. Discussion

In the previous content, the feature recognition module and collision candidate detection module were introduced and demonstrated the effectiveness by a case study. Two groups of comparative experiments are used to prove the feasibility of boundary recognition and the superiority of collision candidate detection in this section.

5.1. Comparison experiment of KDE method with K-means and DBSCAN clustering algorithms

Boundary recognition is a very significant part of the feature recognition module. To verify the results identified by the KDE method, a comparison experiment of the KDE method with K-means and DBSCAN algorithms is set up in this section. The experimental area and AIS data of the comparative experiment are the same as the case study. In Section 4.2.1, we obtained several boundary lines through the KDE method. As shown in Fig. 25(a), the solid lines are the real boundaries of the Sutong bridge, and the dotted lines are the boundaries identified by the KDE method. Fig. 25(b) shows the errors between the two groups of boundaries. The results show that they are coincident, even if there are some

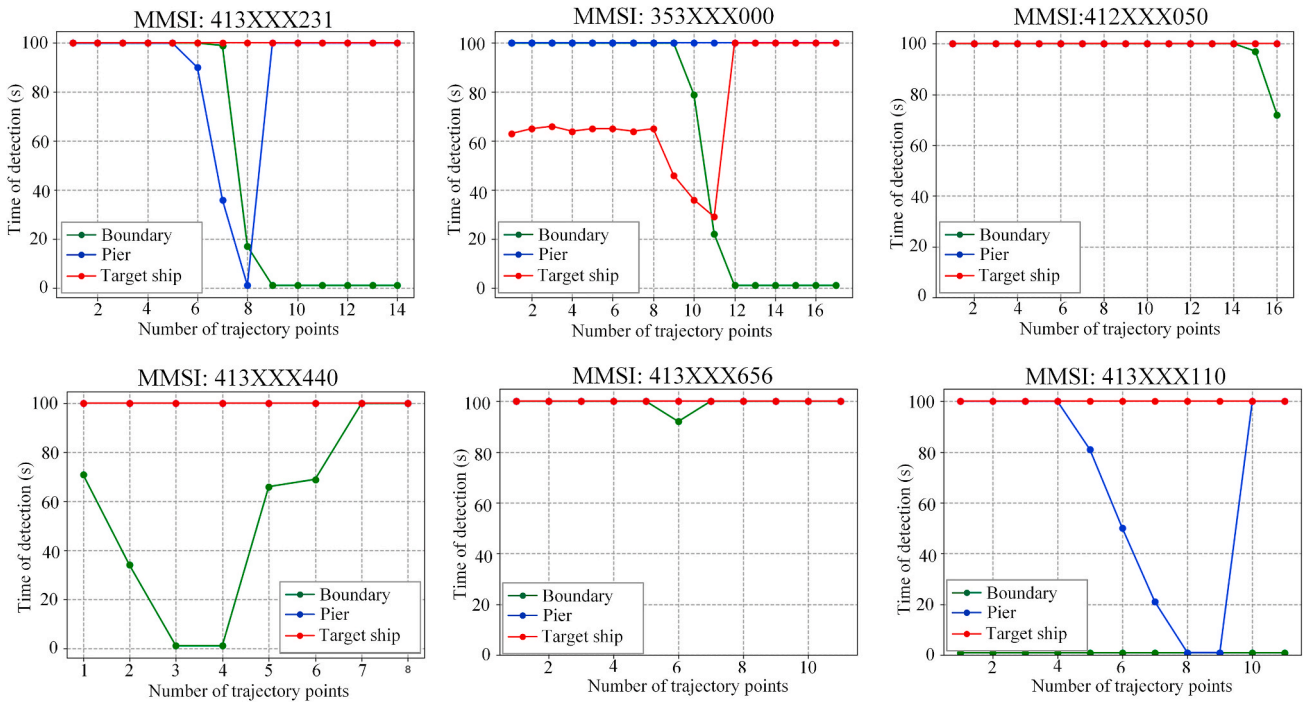

Fig. 24. Result of collision candidate detection.

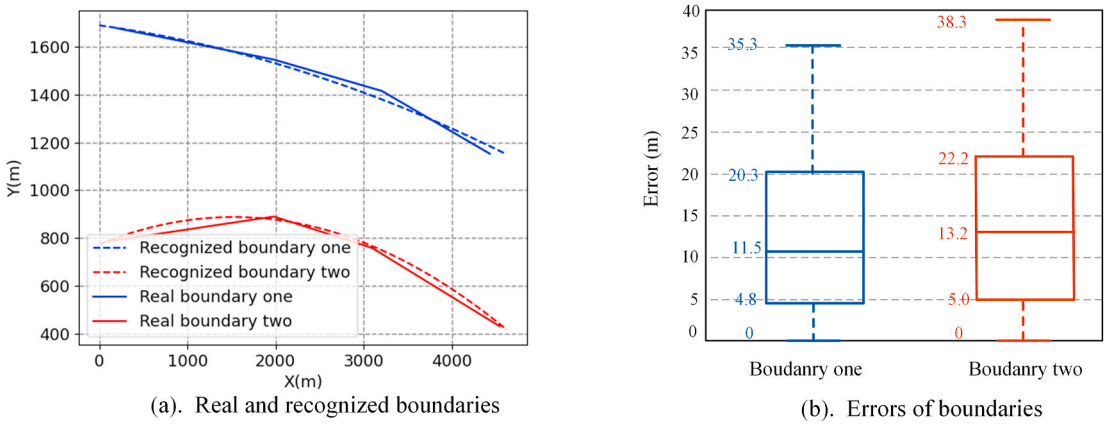

Fig. 25. Comparison results between the recognized and real boundaries.

errors. The maximum error and median error of boundary one are 35.3 m and 11.5 m respectively. The error is generally distributed between 4.8 m and 20.3 m, which can fully meet the navigation practice. The error of boundary 2 is larger than boundary 1, but it is also within the controllable range, and such error can be reduced by more accurate AIS data.

The K-means and DBSCAN clustering algorithms are used to try to identify the boundary lines based on the same data. The similarity functions used by K-means and DBSCAN clustering algorithms are Euclidean distance and Hausdorff distance, as shown in Eq. (19) and Eq. (20), respectively.

$$dist(traj_A, traj_B) = \sqrt{\sum_{d=1}^{D}\left(traj_{A,d} - traj_{B,d}\right)^2} \tag{19}$$

$$\begin{cases} H(traj_A, traj_B) = \max(h(traj_A, traj_B), h(traj_B, traj_A)) \\ h(traj_A, traj_B) = \max\limits_{a \in traj_A}\left[\min\limits_{b \in traj_B} d(a,b)\right] \\ h(traj_B, traj_A) = \max\limits_{b \in traj_B}\left[\min\limits_{a \in traj_A} d(b,a)\right] \end{cases} \tag{20}$$

Where: The $dist(traj_A, traj_B)$ and $H(traj_A, traj_B)$ are Euclidean distance and Hausdorff distance between two trajectories, respectively. The a, b represents the points in the trajectory A and trajectory B, and $d(a,b)$ represents the distance between the two points.

Since the factor of the ship course is not considered in the similarity functions, the ship trajectories are divided into two types of trajectories with a course greater than 180° and less than 180°. The kinematic interpolation is used to unify the number of trajectory points of each trajectory before clustering using the k-means algorithm. Because each type of trajectory includes a deep-water channel and a recommended-water channel, the parameter K of the k-means algorithm is set to 2. The parameters of the DBSCAN clustering algorithm are ε and minPts, which represent the neighborhood radius and the minimum number of

clusters, respectively. The clustering results of the two clustering algorithms are shown in Fig. 26.

It can be seen from the results that neither the K-means clustering algorithm nor the DBSCAN clustering algorithm can distinguish ship trajectories in different channels. Through the comparative experiment, it can be proved that the KDE method is more effective than the K-means and DBSCAN clustering algorithms in finding the channel boundary of the bridge waterways, especially with multiple navigable channels. In many bridge waterways, there are insufficient buoys due to various restrictions. Through this method, the boundaries of the bridge waterways without buoys can be identified, which is very helpful for passing ships and helps to reduce the probability of collision accidents.

5.2. Comparison experiment of the VO method with CPA model and fuzzy theory based model

To further analyze the advantages of the collision candidate detection model, it is compared with the original CPA model and typical fuzzy theory based model. The CPA model consists of DCPA and TCPA, which are widely used in navigation practice. A collision candidate is considered to happen when two conditions are met: 1) DPCA is less than the set threshold; 2) TCPA is less than the set threshold and greater than 0. The collision risk model based on fuzzy theory is one of the most typical indicator-based collision risk models. In this section, the collision risk model based on fuzzy logic proposed by Zhang et al., 2021)(b)) is used to evaluate the collision risk of a ship crossing the bridge waterways. The collision risk factors involved in the model include DCPA, TCPA, relative distance (D), relative bearing angle (β), and the ratio of speed (K). The equation can be expressed as:

$$CRI = 0.40u(DCPA) + 0.367u(TCPA) + 0.167u(D) + 0.033u(\beta) + 0.033u(K) \tag{21}$$

Where: $u(\,)$ represents the function of risk value corresponding to different risk factors, and the details can be referred to Zhang et al. (2021(b)).

We will illustrate the advantages of the VO method over the original CPA model and typical fuzzy theory based model through a group of comparative experiments. As shown in Fig. 27, ship "353XXX000" is an overtaking ship that does not fully comply with the rules of the bridge waterways. It sails out of the established channel after passing the bridge. Ship "412XXX050" is a stand-on ship sailing along the channel in compliance with the rules. The above three models will be used to detect the collision candidate risk of each trajectory point of the ship 353xxx000, respectively.

Fig. 28 shows the results of detecting ship 353XXX000 using three collision candidate detection models. The thresholds of TCPA, DCPA, CRI and t_f are set to 60s, 500 m, 0.6, and 60s respectively. The red and green lines in figure (a) and figure (b) are the CPA values between ship 353XXX000 and ship 412XXX050, and between ship 353XXX000 and the pier, respectively. A collision candidate happened when the point falls in the shaded parts of the figure (a) and figure (b) at the same time. There is no potential collision risk because the conditions cannot be met at any point of the ship 353XXX000. The 9th, 10th and 11th points fall in the shadow area of figure (c), which are identified as collision candidate points with ship 412XXX050 by the fuzzy theory-based model. Moreover, the detection result in figure (d) is consistent with figure (c) if the detection result of the ship and channel boundary (blue line) is removed. Otherwise, the points except for the 1st to 8th are considered collision candidate points in figure (d).

The collision candidate points are determined in different ways among the three models, it is hard to explain which model is more suitable for the bridge waterways only from the results. However, it can be clearly seen that the original CPA method is more complicated in collision candidate identification, because TCPA and DCPA need to meet the trigger conditions at the same time. The results detected by the models based on fuzzy theory and the VO method are relatively easy to understand. Moreover, The CPA and the fuzzy theory-based models are often used to assess the collision candidate between trajectory points and punctate features, such as pier and target ship. But the VO method can be used to detect both collision candidates with punctate targets and collision candidates with linear targets. By comparing and analyzing the results, the VO method adopted in this paper is more suitable for the collision candidate detection of bridge waterways.

5.3. Limitations and further improvements

Despite the advantages mentioned above, the proposed method has still revealed some limitations. Further studies are required to improve the research from the following aspects:

(1) The ship trajectory prediction model needs to be further extended. The current research can only focus on the historical trajectory because it is temporarily impossible to predict the ship trajectory in real-time. If the trajectory prediction of each passing ship can be realized, the research can carry out real time bridge waterways collision candidate detection.

(2) Ship maneuverability and collision avoidance rules are not considered, since the objective of this work is to propose a method to identify the collision candidate of ship encounters in the bridge areas. As the next step of the research, which will focus on the collision avoidance decision-making support tool for ship navigating in the bridge area, such factors should be sophistically considered.

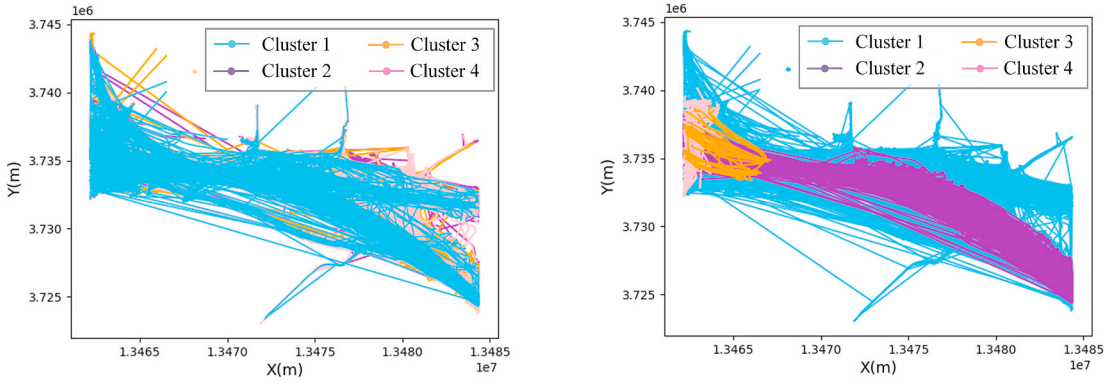

(a) The result of K-means clustering algorithm

(b) The result of DBSCAN clustering algorithm

Fig. 26. The clustering results of the two clustering algorithms.

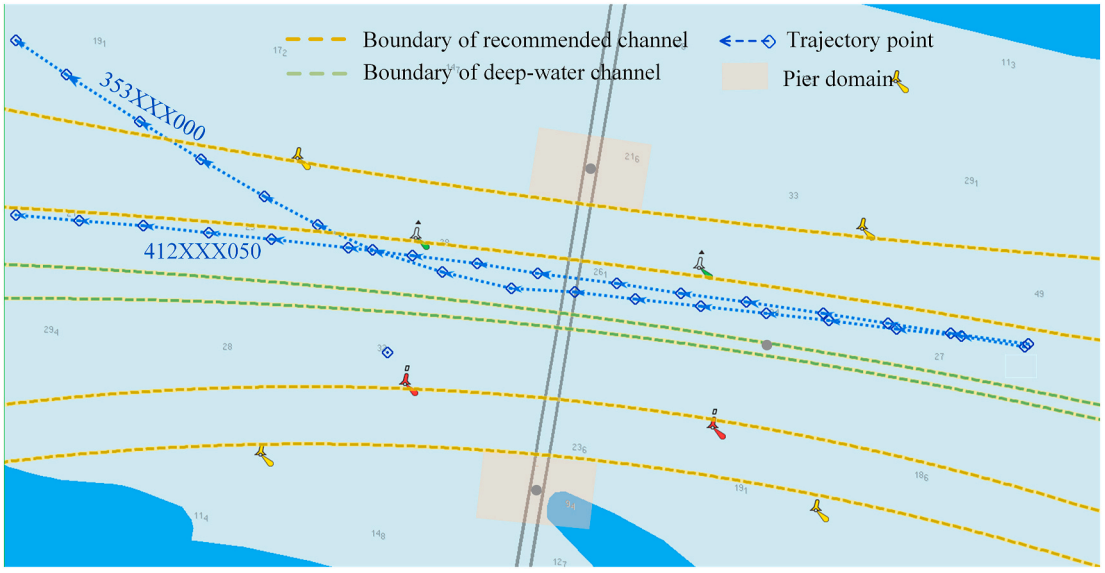

Fig. 27. Trajectories of ship 353XXX000 and ship 412XXX050.

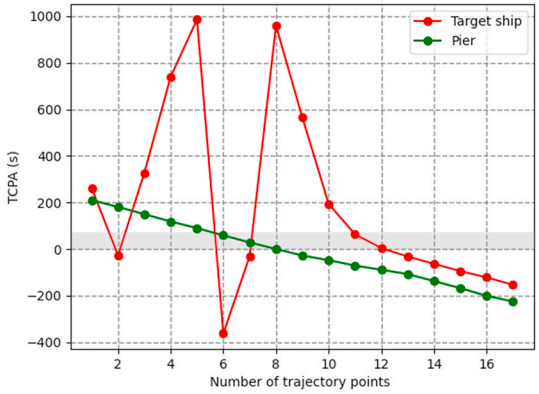

(a) The results of TCPA

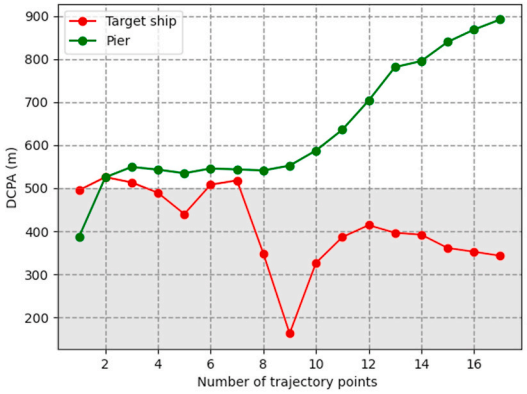

(b) The results of DCPA

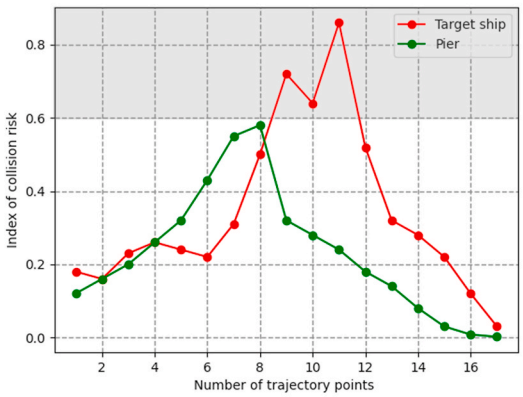

(c) The results detected by fuzzy theory based model

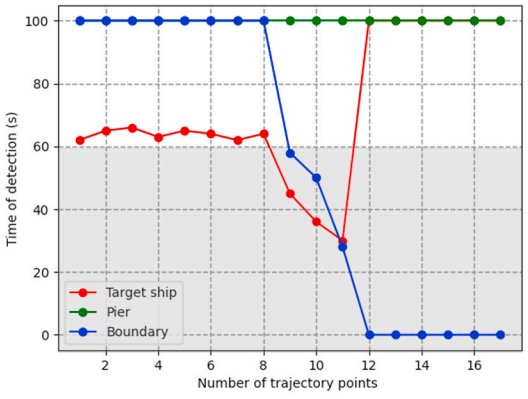

(d) The results detected by VO method

Fig. 28. The results of the comparison experiment.

6. Conclusion

Ship-bridge collision accidents have the potential to cause significant financial loss and injury. Collision candidate detection is one of the effective methods to reduce the probability of ship-bridge collision. In this paper, a collision candidate detection approach for bridge waterways was proposed. The contribution of this paper is two-fold: 1) This paper proposed an approach for collision candidate detection in bridge waterways from the perspective of active anti-collision; 2) The collision candidate detection method proposed in this paper considers the coupling effect of all targets in the bridge waterways. The model design of this paper mainly includes data preprocessing, feature

recognition, and collision candidate detection modules. After decoding, cleaning, and kinematic interpolation of the original AIS data in the data preprocessing module, more accurate data were provided for the latter two modules. The feature recognition module identified the features of the bridge waterways by the KDE method based on preprocessed AIS data. As for the collision candidate detection module, the basic principle of collision candidate and the variation of the equation for different targets are introduced. The above three modules can effectively detect the collision candidates of historical AIS data and contribute to reducing the probability of collision risk in the bridge waterways.

The feasibility and effectiveness of the approach proposed in the paper are proved by analyzing the Sutong bridge waterways. In the case study, one-week data were collected for feature recognition, and six trajectories were randomly selected to perform collision candidate detection. The experimental results show that the approach can successfully identify the features and detect the collision candidate points. The comparative analysis shows that the accuracy of identified features meets the requirements of navigation practice. Compared with conventional collision candidates detection methods, such as the CPA model and the fuzzy theory-based model, the VO method is more suitable for bridge waterways.

Further research on the collision candidate of the bridge waterway is recommended as follows. First, expand the trajectory prediction model and study the real-time collision candidate detection approach of bridge waterways. Secondly, combined with the ship motion model and collision avoidance rules to provide decision support for ships with potential risks. Finally, a complete system is developed, which can realize the real-time transmission of decision support.

CRediT authorship contribution statement

Liang Zhang: Conceptualization, Methodology, Investigation, Formal analysis, Writing – original draft. **Pengfei Chen:** Methodology, Formal analysis, Writing – review & editing, Visualization. **Mengxia Li:** Conceptualization, Methodology, Investigation, Writing – review & editing. **Linying Chen:** Methodology, Formal analysis, Writing – review & editing. **Junmin Mou:** Methodology, Resources, Supervision.

Declaration of competing interest

The authors declare that they have no known competing financial interests or personal relationships that could have appeared to influence the work reported in this paper.

Data availability

Data will be made available on request.

Acknowledgment

The work presented in this study is financially supported by the National Natural Science Foundation of China under grants 52101402, 52001242, and 52271367.

References

AASHTO, 2009. Guide Specifications and Commentary for Vessel Collision Design of Highway Bridges. American Association of State Highway and Transportation Officials, Washington, DC.
Chin, H.C., Debnath, A.K., 2009. Modeling perceived collision risk in port water navigation. Saf. Sci. 47 (10), 1410–1416.
Chen, P., Huang, Y., Mou, J., van Gelder, P.H.A.J., 2018. Ship collision candidate detection method: a velocity obstacle approach. Ocean Eng. 170, 186–198.
Chen, P., Huang, Y., Papadimitriou, E., Mou, J., van Gelder, P.H.A.J., 2020a. An improved time discretized non-linear velocity obstacle method for multi-ship encounter detection. Ocean Eng. 196, 106718.
Chen, P., Huang, Y., Papadimitriou, E., Mou, J., van Gelder, P.H.A.J., 2020b. Global path planning for autonomous ship: a hybrid approach of fast marching square and velocity obstacles methods. Ocean Eng. 214, 107793.
Chen, W., Wang, Y.G., Li, W., Yang, L.M., Liu, J., Dong, X.L., Zhu, H.H., Wang, F., 2021. An adaptive arresting vessel device for protecting bridges over non-navigable water against vessel collision. Eng. Struct. 237.
Davis, 1980. A Computer simulation of marine traffic using domains and arenas[J]. J. Navig. 33, 215, 02.
Debnath, A.K., Chin, H.C., 2009. Navigational traffic conflict technique: a proactive approach to quantitative measurement of collision risks in port waters. J. Navig. 63 (1), 137–152.
Du, D., 2018. Study on the bridge-waters area ship safety collision avoidance navigation system. In: The 30th Chinese Control and Decision Conference (2018 CCDC), vol. 3, pp. 3603–3606.
Du, L., Banda, O.A.V., Huang, Y., Goerlandt, F., Kujala, P., Zhang, W., 2021. An empirical ship domain based on evasive maneuver and perceived collision risk. Reliab. Eng. Syst. Saf. 213, 107752.
Fujii, Y., Tanaka, K., 1971. Traffic capacity. J. Navig. 24, 543–552, 04.
Fan, W., Yuan, W., Chen, B., 2015. Steel Fender limitations and improvements for bridge protection in ship collisions. J. Bridge Eng. 20 (12), 06015004.
Fang, H., Mao, Y., Liu, W., Zhu, L., Zhang, B., 2016. Manufacturing and evaluation of large-scale composite bumper system for bridge pier protection against ship collision. Compos. Struct. 158, 187–198.
Goodwin, 1975. A statistical study of ship domains. J. Navig. 28 (3), 328–344.
Gil, M., Montewka, J., Krata, P., Hinz, T., Hirdaris, S., 2020. Determination of the dynamic critical maneuvering area in an encounter between two vessels: operation with negligible environmental disruption. Ocean Eng. 213, 107709.
Guo, S., Mou, J., Chen, L., Chen, P., 2021. Improved kinematic interpolation for AIS trajectory reconstruction. Ocean Eng. 234, 109256.
Hansen, M., Jensen, T., Melchild, K., Rasmussen, F.M., Ennemark, F., 2013. Empirical ship domain based on AIS data. J. Navig. 66 (6), 931–940.
ITU, 2010. Technical Classifications of Recommendations ITU-M. 1371-4. Technical Characteristics for an Automatic Identification System Using Time-Division Multiple Access in the VHF Maritime Mobile Band.
Jiang, H., Chorzepa, M.G., 2015. Evaluation of a new FRP fender system for bridge pier protection against vessel collision. J. Bridge Eng. 20, 05014010.
Jiang, H., Chorzepa, M.G., 2016. Case study: evaluation of a floating steel fender system for bridge pier protection against vessel collision. J. Bridge Eng. 21 (11), 05016008.
Larsen, O.D., 1993. Ship Collision with Bridges: the Interaction between Vessel Traffic and Bridge Structures. International Association of Bridge and Structural Engineering.
Liu, Y., Xiao, Y., 2014. Risk degree of ship-bridge collision based on theory of ship collision avoidance. International Journal of Control and Automation 7 (11), 303–316.
Liu, J., Feng, Z., Li, Z., Wang, M., Wen, L.R., 2016. Dynamic ship domain models for capacity analysis of restricted water channels. J. Navig. 69, 481–503.
Li, M., Mou, J., Liu, R., Chen, P., Dong, Z., He, Y., 2019. Relational model of accidents and vessel traffic using AIS data and GIS: a Case study of the western port of ShenZhen city. J. Mar. Sci. Eng. 7 (6), 2019.
Lu, N., Liang, M., Zheng, R., Liu, R.W., 2020. Historical AIS data-driven unsupervised automatic extraction of directional maritime traffic networks. In: 2020 IEEE 5th International Conference on Cloud Computing and Big Data Analytics (ICCCBDA), pp. 7–12.
Liu, K., Yuan, Z., Xin, X., Yang, Z., Zhang, J., Wang, W., 2021. Conflict detection method based on dynamic ship domain model for visualization of collision risk Hot-Spots. Ocean Eng. 242, 110143.
Li, M., Mou, J., Chen, L., He, Y., Huang, Y., 2021. A rule-aware time-varying conflict risk measure for MASS considering maritime practice. Reliab. Eng. Syst. Saf. 215, 107816.
Mou, J., Tak, c.v.d., Ligteringen, H., 2010. Study on collision avoidance in busy waterways by using AIS data. Ocean Eng. 37, 483–490.
Mou, J., Li, M., Hu, W., Zhang, X., Gong, S., Chen, P., He, Y., 2020. Mechanism of dynamic automatic collision avoidance and the optimal route in multi-ship encounter situations. J. Mar. Sci. Technol. 26 (1), 141–158.
Ma, W., Zhu, Y., Grifoll, M., Liu, G., Zheng, P., 2022. Evaluation of the effectiveness of active and passive safety measures in preventing ship-bridge collision. Sensors 22 (8), 2857.
Pedersen, P.T., Chen, J., Zhu, L., 2020. Design of bridges against ship collisions. Mar. Struct. 74, 102810.
Rutkowski, G., 2021. Analysis of a practical method for estimating the ship's best possible speed when passing under bridges or other suspended obstacles. Ocean Eng. 225, 108790.
Shu, W., Yu, M., 2007. Development of collision avoidance system by using expert system and search algorithm. Ship. Technol. 29 (4), 121–124.
Svensson, H., 2009. Protection of bridge piers against ship collision. Steel Construct. 2 (1), 21–32.
Sha, Y., Amdahl, J., Liu, K., 2019. Design of steel bridge girders against ship forecastle collisions. Eng. Struct. 196, 109277.
Sha, Y., Amdahl, J., Dørum, C., 2021. Numerical and analytical studies of ship deckhouse impact with steel and RC bridge girders. Eng. Struct. 234, 111868.
Wang, N., 2013. A novel analytical framework for dynamic quaternion ship domains. J. Navig. 66, 265–281.
Wu, B., Yip, T.L., Yan, X., Guedes Soares, C., 2019. Fuzzy logic based approach for ship-bridge collision alert system. Ocean Eng. 187, 106152.
Xiao, F., Ligteringen, H., van Gulijk, C., Ale, B., 2015. Comparison study on AIS data of ship traffic behavior. Ocean Eng. 95, 84–93.
Xue, J., Wu, C., Chen, Z., Chen, X., 2017. A novel estimation algorithm for interpolating ship motion. 2017 4th International Conference on Transportation Information and Safety (ICTIS). IEEE, pp. 557–562.

Yoo, S.L., 2018. Near-miss density map for safe navigation of ships. Ocean Eng. 163, 15–21, 2018.
Zhang, W., Goerlandt, F., Montewka, J., Kujala, P., 2015. A method for detecting possible near miss ship collisions from AIS data. Ocean Eng. 107, 60–69.
Zhao, L., Shi, G., 2018. A method for simplifying ship trajectory based on improved Douglas–Peucker algorithm. Ocean Eng. 166, 37–46.
Zhang, X., He, Y., Tang, R., Mou, J., Gong, S., 2018. A novel Method for reconstruct ship trajectory using raw AIS Data. In: 2018 3rd IEEE International Conference on Intelligent Transportation Engineering (ICITE). IEEE, pp. 192–198.
Zhu, L., Liu, W., Fang, H., Chen, J., Zhuang, Y., Han, J., 2019. Design and simulation of innovative foam-filled lattice composite bumper system for bridge protection in ship collisions. Composites Part B 157, 24–35.
Zhang, L., Meng, Q., 2019. Probabilistic ship domain with applications to ship collision risk assessment. Ocean Eng. 186, 106130.
Zhang, D., Zhang, Y., Zhang, C., 2021a. Data mining approach for automatic ship-route design for coastal seas using AIS trajectory clustering analysis. Ocean Eng. 236, 109535.
Zhang, M., Montewka, J., Manderbacka, T., Kujala, P., Hirdaris, S., 2021b. A big data analytics method for the evaluation of ship - ship collision risk reflecting hydrometeorological conditions. Reliab. Eng. Syst. Saf. 213, 107674.